OPEN BIOLOGY

royalsocietypublishing.org/journal/rsob

Research

Cite this article: Cimmino TP, Pagano E, Stornaiuolo M, Esposito G, Ammendola R, Cattaneo F. 2023 Formyl-peptide receptor 2 signalling triggers aerobic metabolism of glucose through Nox2-dependent modulation of pyruvate dehydrogenase activity. *Open Biol.* **13**: 230336.
https://doi.org/10.1098/rsob.230336

Received: 13 September 2023
Accepted: 20 September 2023

Subject Area:
biochemistry

Keywords:
formyl peptide receptors, NADPH oxidase, reactive oxygen species, tyrosine kinase receptor transactivation, glucose metabolism, Warburg effect

Author for correspondence:
Fabio Cattaneo
e-mail: fabio.cattaneo@unina.it

Electronic supplementary material is available online at https://doi.org/10.6084/m9.figshare.c.6875416.

THE ROYAL SOCIETY PUBLISHING

Formyl-peptide receptor 2 signalling triggers aerobic metabolism of glucose through Nox2-dependent modulation of pyruvate dehydrogenase activity

Tiziana Pecchillo Cimmino[1], Ester Pagano[2], Mariano Stornaiuolo[2], Gabriella Esposito[1], Rosario Ammendola[1] and Fabio Cattaneo[1]

[1]Department of Molecular Medicine and Medical Biotechnology, School of Medicine and [2]Department of Pharmacy, School of Medicine, University of Naples Federico II, 80131 Naples, Italy

TPC, 0000-0003-0545-2981; EP, 0000-0003-2872-1734; MS, 0000-0003-2200-5083; GE, 0000-0002-4255-7312; RA, 0000-0003-1655-8028; FC, 0000-0002-5833-8333

The human formyl-peptide receptor 2 (FPR2) is activated by an array of ligands. By phospho-proteomic analysis we proved that FPR2 stimulation induces redox-regulated phosphorylation of many proteins involved in cellular metabolic processes. In this study, we investigated metabolic pathways activated in FPR2-stimulated CaLu-6 cells. The results showed an increased concentration of metabolites involved in glucose metabolism, and an enhanced uptake of glucose mediated by GLUT4, the insulin-regulated member of GLUT family. Accordingly, we observed that FPR2 transactivated IGF-IRβ/IRβ through a molecular mechanism that requires Nox2 activity. Since cancer cells support their metabolism via glycolysis, we analysed glucose oxidation and proved that FPR2 signalling promoted kinase activity of the bifunctional enzyme PFKFB2 through FGFR1/FRS2- and Akt-dependent phosphorylation. Furthermore, FPR2 stimulation induced IGF-IRβ/IRβ-, PI3K/Akt- and Nox-dependent inhibition of pyruvate dehydrogenase activity, thus preventing the entry of pyruvate in the tricarboxylic acid cycle. Consequently, we observed an enhanced FGFR-dependent lactate dehydrogenase (LDH) activity and lactate production in FPR2-stimulated cells. As LDH expression is transcriptionally regulated by c-Myc and HIF-1, we demonstrated that FPR2 signalling promoted c-Myc phosphorylation and Nox-dependent HIF-1α stabilization. These results strongly indicate that FPR2-dependent signalling can be explored as a new therapeutic target in treatment of human cancers.

1. Introduction

G protein-coupled receptors (GPCRs) and tyrosine kinase receptors (TKRs) play critical roles in health and disease and represent the major classes of cell surface receptors. GPCRs bind a structurally diverse range of ligands [1] which trigger downstream signalling via heterotrimeric G protein dissociation (Gα and G$\beta\gamma$ subunits) [2]. TKRs bind growth factors which typically induce dimerization of receptor monomers triggering trans-autophosphorylation of COOH-terminal tyrosine residues that act as recruitment sites for intracellular adaptor proteins. Typically, TKR-mediated signalling is a driver for cell proliferation, migration and survival.

GPCR-mediated TKR transactivation represents a molecular mechanism necessary to increase the number and range of cellular signalling networks, by integrating the diversity of GPCRs and their ligands with the large signalling networks related to TKRs [3]. Trans-phosphorylation has been implicated in physiological and pathophysiological processes and has been observed for

several receptor pairings in many cell types [4,5]. As involved molecular mechanisms and signalling effectors can vary with receptor couple [6], the GPCR/TKR interactions may be considered attractive new targets for drug discovery programmes.

Stimulation of several GPCR induces a low increase of NADPH oxidase (Nox)-dependent reactive oxygen species (ROS) concentration, that act as signalling molecules in several cellular processes, such as phosphorylation of kinases, activation of transcription factors and TKR transactivation [7–14]. The classical NADPH oxidase of phagocytes consists of five subunits: $p67^{phox}$, $p47^{phox}$, $p40^{phox}$, $p22^{phox}$ and the catalytic subunit $gp91^{phox}$. Members of this family, identified in several nonphagocytic cells, are homologues of the catalytic subunit $gp91^{phox}$ and are named Nox1, Nox3, Nox4, Nox5, Duox1 and Duox2. Nox2 is also known as $gp91^{phox}$. Nox activity is controlled by $p47^{phox}$ and $p67^{phox}$ regulatory subunits, their homologues NOXO1 and NOXA1, or DUOXA1 and 2. Moreover, the GTPase Rac modulates the activity of several of these enzymes [15]. Nox1, Nox2, Nox3 and Nox5 are transmembrane proteins that transport electrons across biological membranes to reduce oxygen to superoxide. Nox4, Duox1 and Duox2 do not produce superoxide, but hydrogen peroxide [7–14]. Members of the Nox family have been identified as the major sources of ROS generation in cancer cells [16] and, among these, Nox2 is strongly expressed in several epithelial cancer cells, such as lung [17], ovarian [18], breast [19], cervical [20] and prostate cells [21]. ROS that are generated by Nox enzymes in non-phagocytic tissues are well documented second messengers in a variety of signalling pathways in several cell types [22]. Molecular mechanisms through which ROS modulate cell signalling depend on their capacity to oxidize cysteine residues within proteins, which can function as redox sensors and transducers of ROS-primed signalling [23]. Therefore, cells can sense ROS to variable levels through the reversible oxidation of cysteine residues allowing a gradual response to intracellular ROS concentrations.

The human formyl-peptide receptor (FPR) family is clustered on chromosome 19 and encodes three Class A GPCRs involved in neutrophil chemotaxis and in innate immune responses, through recognition of pathogen-associated molecular patterns (PAMPs) and damage-associated molecular patterns (DAMPs) [24]. FPR2, a member of this family, is highly expressed in myeloid cells and in cells of diverse origin [25], as well as on the nuclear membrane of CaLu-6 and AGS cells [26]. FPR2 is activated by an array of ligands including proteins, peptides and lipids. Most of them, besides inducing chemotaxis, also stimulate pro-inflammatory processes, pro-resolving or anti-inflammatory pathways [27], depending on the nature of the agonist and on the different receptor domains they used [28,29]. The switch between pro-inflammatory and anti-inflammatory responses is due to conformational changes of FPR2 upon ligand binding [29]. The peptide WKYMVm, annexin A1 (ANXA1) and lipoxin A4 (LXA4) are well-known anti-inflammatory FPR2 ligands [30–32]. On the other hand, serum-amyloid alpha (SAA) and β-amyloid act as pro-inflammatory agonists on FPR2 [33]. FPR2 contributes to detrimental effects in cancer progression. In fact, invasion of ovarian cancer cells requires FPR2 activation by the cathelicidin LL-37 [34], the Hp(2-20) peptide, that efficiently binds FPR2, promotes the migration and proliferation of gastric cancer cells [35] and ANXA1 stimulates the development and progression of astrocytoma [36]. However, the role of FPR2 in cancer progression is still controversial and seems related to the nature of its ligands and of cell type, as demonstrated by the observation that LXA4 attenuates pancreatic cell invasion [37].

FPR2 stimulation triggers the activation of several protein kinases and, in turn, the phosphorylation of several cytosolic signalling proteins [13,25,38] involved in the modulation of proliferation, differentiation, migration, communication, and other critical intracellular functions [39]. FPR2-dependent phosphorylated molecules include also non-signalling proteins, such as the cytosolic subunits $p47^{phox}$ and $p67^{phox}$ of NADPH oxidase, whose phosphorylation is required for the full activity of the NADPH oxidase complex [12,14].

Protein kinases mediate a network of highly complex signals. Many proteins, including TKRs [3], are phosphorylated and the main mechanism of regulation is represented by the switch 'phosphorylation/dephosphorylation', in which protein phosphatases (PTPases), through the reversible oxidative inhibition of reactive cysteine residues, play a crucial role [40–42]. We previously demonstrated that FPR1 and FPR2 stimulation induces ROS-dependent TKR transactivation, as well as the phosphorylation and nuclear translocation of regulatory transcriptional factors [9–11,14,43]. Protein kinases and PTPases act synergistically and their impaired regulation or activation is responsible of several human diseases. Multiple phospho-sites, identified in both protein kinases and phosphatases, contribute decisively to expand the repertory of molecular mechanisms of regulation or for fine-tuning of switch properties [44].

By using a phospho-proteomic approach we previously demonstrated that FPR2 stimulation induces redox-regulated phosphorylation of numerous proteins [38,44]. We classified FPR2-dependent phosphorylated proteins according to their known or putative functions and this analysis revealed that most of them participated in metabolic processes. About 33% of the proteins of this group is involved in biosynthetic processes and the remaining 67% of proteins is involved in cellular metabolic processes, including primary metabolism [38]. We also demonstrated that the binding of specific FPR2 agonists enhances the non-oxidative phase of pentose phosphate pathway (PPP), improves the expression of the ASCT2 glutamine transporter and induces the de novo synthesis of pyrimidine nucleotides [45].

Herein, we apply a metabolomic approach to analyze the metabolic pathways activated in human CaLu-6 epithelial carcinoma cell line, following stimulation of FPR2 with the WKYMVm peptide or ANXA1. Obtained results prove that the agonist-mediated stimulation of the receptor triggers intracellular redox signalling pathways involved in glucose uptake and aerobic metabolism of glucose typical of the Warburg effect.

2. Material and methods

2.1. Cell culture and reagents

CaLu-6, A549 (ATTC, Manassas, VA, USA) and p22phox $^{Crispr/Cas9}$ CaLu-6 cells were cultured in Dulbecco's modified Eagle's medium (DMEM) supplied with 10% fetal bovine serum (FBS) (Invitrogen Corp., Carlsbad, CA, USA) at 37°C and 5% CO_2. Cells were grown to 70% confluence, serum

starved for 24 h and stimulated or not with 10 µM WKYMVm (Primm, Milan, Italy) or 10 nM ANXA1 for various times, as indicated in the figures. CaLu-6 cells were also preincubated with WRWWWW (WRW4) (Primm, Milan, Italy) for 15 min at a final concentration of 10 µM, or with apocynin (Sigma Chemical, St Louis, MO, USA) for 2 h at a final concentration of 5 mM, or with PP2 or with PP3 (Calbiochem, La Jolla, CA, USA) for 45 min at the final concentration of 10 µM, or with GSK1904529A (MedChemExpress, Monmouth Junction, NJ, USA) for 2 h at the final concentration of 3 µM, or with LY2874455 (MedChemExpress, Monmouth Junction, NJ, USA) for 2 h at the final concentration of 5 µM, or with AG1478 (Calbiochem, La Jolla, CA, USA) for 60 min at the final concentration of 10 µM, or with wortmannin (Calbiochem, La Jolla, CA, USA) for 60 min at the final concentration of 0.5 µM, or with LY294002 (Calbiochem, La Jolla, CA, USA) for 60 min at the final concentration of 10 µM, before stimulation with 10 µM WKYMVm or 10 nM ANXA1.

2.2. p22phox$^{crispr/Cas9}$ double-nickase CaLu-6 cells

p22phox$^{Crispr/Cas9}$ cells were generated by transfecting CaLu-6 cells with Double Nickase Plasmid or with a Double Nickase Plasmid control (Santa Cruz Biotechnology, Irvine, CA, USA) following the manufacturer's instructions, as previously described [25]. Positive selection of CaLu-6-transfected cells was performed in medium containing puromycin for 5 days. Single clones were isolated, cultured separately, and tested by western blotting to analyze p22^{phox} expression (data not shown). p22^{phox} knockout clones were collected in order to obtain p22phox$^{Crispr/Cas9}$ CaLu-6 cells.

2.3. Metabolomic analysis by liquid chromatography–mass spectrometry

Metabolomic analysis by LC-MS was performed in growing and in 24 h serum starved CaLu-6 cells stimulated or not with WKYMVm in presence or absence of WRW4. Briefly, 2×10^4 cells were plated in 48-multiwell plate and the day after were serum-starved for 24 h before the treatments. Cell monolayers were rinsed in cold water and then lysed in 400 µl of a 1:1 prechilled MetOH:H_2O solution. The samples were vortex-mixed, kept on ice for 20 min, and centrifuged again at 10 000 × *g*, at 4°C for 10 min. The collected supernatant was dried in a SpeedVac concentrator system (Thermo Scientific), operated at room temperature. Dried supernatants were reconstituted with 125 µl of methanol/acetonitrile/water (50:25:25). Extracted metabolites were analysed using an ACQUITY UPLC system online coupled to a Synapt G2-Si QTOF-MS (Waters Corporation, Milford, MA, USA) in positive and negative modes in the following settings: reverse-phase ACQUITY UPLC CSH C18 (1.7 µm, 100 × 2.1 mm^2) column (Waters), 0.3 ml min^{-1} flow rate, mobile phases composed of acetonitrile/H_2O (60 : 40) containing 0.1% formic acid and 10 mM ammonium formate (phase A), and isopropanol/acetonitrile (90 : 10) containing 0.1% formic acid and 10 mM ammonium formate (phase B). Peak detection, metabolite identification and quantitation were performed as previously described [46], fitting experimental data with internal standard and calibration curves. Data analysis was conducted and heatmaps were generated with the on-line software MetaboAnalyst (https://www.metaboanalyst.ca), as previously reported [47,48] (electronic supplementary material, table S1).

2.4. 2-NBDG glucose uptake assay on CaLu-6 cells

CaLu-6 cells were plated (5×10^3 per well) in a black, clear bottom, 96-well microtiter plate (Perkin Elmer, Waltham, USA) in a final volume of 100 µl per well of culture medium. After 24 h the culture medium was carefully removed and replaced with 100 µl of HBSS containing 100 µM 2-deoxyglucose (2-DG), 0.4 g l^{-1} BSA, and 1.3 mM $CaCl_2$ (in the absence of any growth factors or FBS) and were incubated with WKYMVm at the final concentration of 10 µM for the indicated times in presence or absence of WRW4. Plates were incubated at 37°C for 1 h. Treatments were performed in triplicate and the results are the mean of three independent experiments. Medium was replaced with the same HBSS supplemented with 100 µM 2-DG and 6 µM 2-(*N*-(7-nitrobenz-2-oxa-1,3-diazol-4-yl)amino)-2-deoxyglucose (2-NBDG). Plates were incubated with the fluorescent probe for 45 min and then washed twice in PBS. Uptake of 2-NDBG was measured in a Perkin Elmer Envision 2105 multiplate reader (Perkin Elmer), using the inbuilt monochromator and the following parameters: λ excitation 471 nm, λ emission 529 nm, and monochromator cut off 360 nm. After the measurement of 2-NDBG, cells were fixed in 3.7% paraformaldehyde for 30 min to be then permeabilized in 0.1% Triton X-100 in PBS and stained with the nuclear dye DAPI (30 µM). This second fluorescence measurement correlates with the total number of cells in each well and was used for normalization. DAPI fluorescence was measured using the following parameters: λ excitation 351 nm and λ emission 450 nm. Data analysis for glucose uptake is reported as the ratio between intracellular 2-NDBG fluorescence and DAPI fluorescence ± s.d.

2.5. Protein extraction and western blot

Proteins were purified from 24 h serum-starved CaLu-6 or p22phox$^{Crispr/Cas9}$ CaLu-6 cells stimulated or not with 10 µM WKYMVm, in the presence or absence of selective inhibitors, as described above. Whole lysates were obtained by scraping cells with ice cold RIPA buffer (50 mM Tris–HCl, pH 7.4, 150 mM NaCl, 1% NP-40, 1 mM EDTA, 0.25% sodium deoxycholate, 1 mM NaF, 10 µM Na_3VO_4, 1 mM phenyl-methyl-sulfonyl-fluoride, 10 µg ml^{-1} aprotinin, 10 µg ml^{-1} pepstatin, 10 µg ml^{-1} leupeptin), as previously described [49].

Membrane lysates were purified as mentioned above [26]. Cells were lysed in hypotonic buffer containing 10 mM Tris–HCl, 1 mM $CaCl_2$, 150 mM NaCl, 1 mM phenyl-methyl-sulfonyl-fluoride, and a protease inhibitor cocktail (10 µg ml^{-1} aprotinin, 10 µg ml^{-1} pepstatin, and 10 µg ml^{-1} leupeptin) (Buffer II) and centrifuged at 400 × *g* for 10 min at 4°C, in order to obtain a cytosolic and a membrane fraction. Membrane fraction was incubated overnight at 4°C in constant agitation with a buffer containing 125 mM Tris–HCl, 1 mM phenyl-methyl-sulfonyl-fluoride, 1% Triton X100, and the protease inhibitor cocktail (Buffer II).

Bio-Rad protein assay was used to determine protein concentrations (BioRAD, Hercules, CA, USA). Western blot

analysis on whole or membrane lysates was performed as previously described [50].

Anti-tubulin (SC-8035), anti-GAPDH (SC-47724), anti Na/K ATPase (SC-48345), anti-GLUT4 (SC-53566) and anti-phospho-c-Myc (S62) (SC-8000-R) antibodies were purchased from Santa Cruz Biotechnology (Irvine, CA, USA). Anti-phospho-IGF-IR (Y1131/1146), anti-phospho-PFKFB2 (S483), anti-phospho-FRS2 (Y436), anti-phospho-PDH (S293), anti-phospho-LDH (Y10), and anti-phospho-c-Src (Y416) were from Cell Signalling Technology (Denvers, MA, USA). Anti-HIF1α (NB100–105) was from Novus Biologicals (Centennial, CO, USA). Goat-anti-mouse (bs-0296G-HRP) and goat-anti-rabbit (bs-0295G-HRP) were from Bioss Antibodies (Woburn, MA, USA). Proteins were visualized by enhanced chemiluminescence reagent (Amersham Biosciences, Little Chalfont, Buckinghamshire, UK) and were quantified using densitometry (Chemidoc, Bio-Rad). Each experiment with relative densitometric quantification was separately repeated at least three times.

2.6. Lactate assay

Lactate concentration was measured in cell culture medium of CaLu-6 cells by Lactate-Glo Assay (Promega) following the manufacturer's instructions. Briefly, 1.5×10^4 cells were seeded in 96-well plate. The day after, cells were serum-starved for 24 h, preincubated or not with 10 µM WRW4 for 15 min and then stimulated or not with 10 µM WKYMVm for 24 h. Five microlitres of medium was removed for each experimental point and diluted in 95 µl of PBS. For each experimental point, 50 µl of diluted medium was transferred to a 96-well assay plate and 50 µl of lactate detection reagent was added. Assay plate was shaken for 1 min to mix the reagents and incubated for 60 min at room temperature before recording luminescence. DMEM was used as a negative control. Luminescence was read with a Synergy H1 microplate reader (BioteK, VT, USA). Results are the mean of three independent experiments and, in each of these, every experimental point was analysed in triplicate.

2.7. Seahorse XF analysis

Extracellular acidification rate (ECAR) was measured by using the Seahorse XF Glycolytic Rate Assay Kit (Agilent, CA, USA). Calu-6 cells, cultured as described above, were seeded in the XF-24 cell culture plates at 20 000 cells per well, allowed to attach overnight and serum-starved for 24 h. Cells were incubated with 10 µM WKYMVm for 24 h followed by Seahorse assay. Then, medium was changed to Seahorse XF DMEM medium pH 7.4 (Agilent), supplemented with 25 mM glucose, 4 mM L-glutamine and 2 mM pyruvate, and allowed to equilibrate for 1 h in a CO_2-free incubator at 37 °C. Real time measurement of ECAR was performed using an XF-24 Analyzer (Agilent).

2.8. Statistical analysis

Statistical analyses were evaluated by unpaired *t*-test to compare the mean of two independent groups of experiments or by one-way analysis of variance (ANOVA). GraphPad Prism 7 (GraphPad Software Inc., San Diego, CA, USA) was used to compare more than two experiments. All data reported are representative of at least three or more independent experiments and are expressed as means ± standard error mean (SEM). A p value of less than 0.05 was considered to be statistically significant.

3. Results

3.1. FPR2 stimulation induces glucose uptake and increases concentration of metabolites involved in glucose metabolism

We started profiling the metabolic response of CaLu-6 cells upon stimulation with WKYMVm. Compared to untreated cells, we observed an increased concentration of metabolites involved in glucose metabolism, such as glucose 6-phosphate, fructose 1,6-bis-phosphate (F1,6BP), glyceraldheide 3-phosphate (GA3P) and lactate (figure 1*a*). This increase was prevented by the preincubation with the FPR2 antagonist WRW4 (figure 1*a*), suggesting that FPR2 stimulation activated glucose oxidation via glycolysis. In this metabolic pathway, glucose is catabolized to pyruvate with production of 2 molecules of ATP and reduction of 2 mol of NAD^+ to NADH per mole of glucose. Pyruvate, in aerobic conditions, is transported into mitochondria, where pyruvate dehydrogenase complex (PDC) catalyses its oxidative decarboxylation into acetyl-coenzyme A (CoA). This can feed the tricarboxylic acid (TCA) cycle and, in turn, the mitochondrial electron transport chain to produce energy. Pyruvate can be also reduced to lactate by a reaction catalysed by lactate dehydrogenase (LDH), and in our metabolomic analysis we interestingly observed that level of lactate increased in FPR2-stimulated cells (figure 1*a*). In cancer cells, this reaction defines the aerobic utilization of glucose typical of the Warburg effect [51].

Therefore, we evaluated the ability of the FPR2 agonist to stimulate glucose uptake in CaLu-6 cells. Treatment with 10 µM WKYMVm significantly increased glucose consumption in a time-dependent manner, when compared to control cells (figure 1*b*); this effect was prevented by pre-incubation with WRW4, before FPR2 stimulation (figure 1*c*). This result strongly suggests that WKYMVm-induced glucose uptake occurs through FPR2 activation. Enhanced glucose utilization is a known hallmark of cancer cells, which need glucose for energy production. Glucose uptake is mediated by members of transmembrane glucose transporter family, which include facilitative glucose transporters (GLUTs), sodium-glucose co-transporters (SGLTs), and transporters of the SWEET family, largely represented in plants [52]. The GLUT family includes 14 known transporters which are divided into three classes according to their structure. GLUT1 is upregulated in cancer by Src, Ras, Myc and Akt [53–56], and it is repressed by the tumor suppressor p53 [57]. GLUT4 is the insulin-regulated member of this family [58,59] and it is expressed in several cancer cells [60–62].

We analysed incorporation of GLUT1 and GLUT4 onto cell surface and observed that WKYMVm stimulation for different time spans induces GLUT4, but not GLUT1 (data not shown), membrane localization (figure 1*d*), which was prevented by WRW4 (figure 1*e*). In several experimental systems GLUT4 transport to the plasma membrane is regulated by the insulin-stimulated phospatidylinositol 3-kinase (PI3K)/Akt signalling pathway [63].

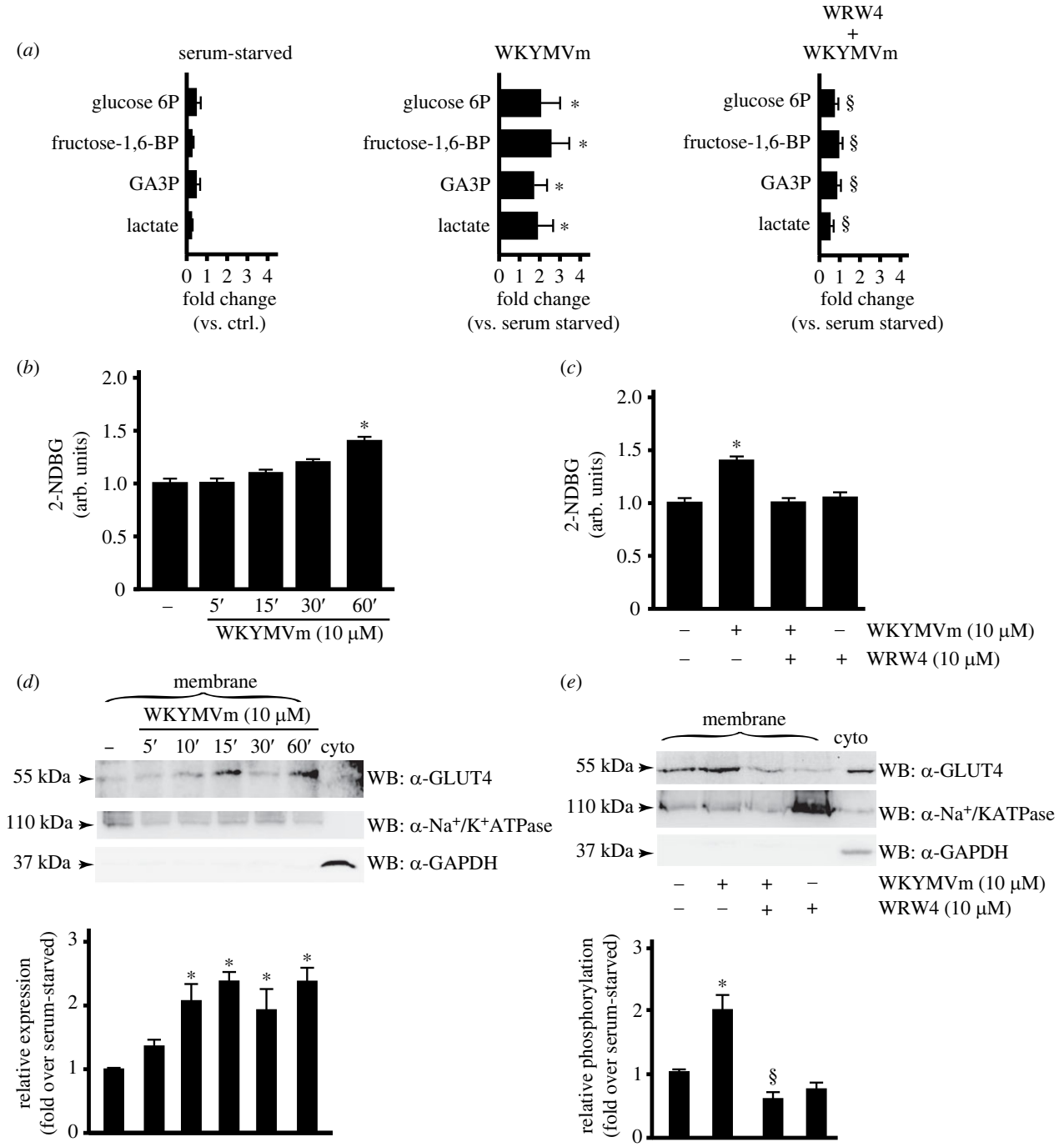

Figure 1. FPR2 stimulation enhances glucose metabolism. (*a*) FPR2-dependent modulation of metabolites involved in glucose metabolism. Growing cells (ctrl) were serum-starved for 24 h and then stimulated or not with 10 µM WKYMVm for 1 h in the presence or absence of 10 µM WRWWWW (WRW4). Metabolomic analysis was performed as described in Material and methods. (*b*,*c*) FPR2 stimulation induces glucose uptake. CaLu-6 cells were grown until reaching 80% of confluence, exposed to 100 µM 2-NDBG and incubated with WKYMVm at final concentration of 10 µM for the indicated times, in the presence or absence of WRW4. Uptake of 2-NDBG was measured in a Perkin Elmer Envision 2105 multiplate reader. Results are the mean of three independent experiments in which each point was analysed in triplicate. *$p < 0.05$ compared to unstimulated cells. (*d*,*e*) GLUT4 membrane translocation depends on FPR2 activation. CaLu-6 cells were serum-starved for 24 h and (*d*) stimulated for 5, 10, 15, 30 or 60 min with WKYMVm, or pretreated with (*e*) WRW4 before stimulation. Sixty micrograms of membranes lysates was immunoblotted with anti-GLUT4 antibody (α-GLUT4). Anti-Na^+/K^+ATPase antibody (α-Na^+/K^+ATPase) was used as a control for protein loading. Sixty micrograms of a cytosolic fraction (Cyto) was loaded and an anti-GAPDH antibody (α-GAPDH) was used as a control of cytosolic proteins. Data are representative of five independent experiments. *$p < 0.05$ compared to unstimulated cells. $^{§}p < 0.05$ compared to WKYMVm-stimulated cells. Glucose 6P: glucose 6-phosphate; fructose 1,6-BP: fructose 1,6-bis-phosphate; GA3P: glyceraldheide 3-phosphate.

3.2. FPR2 signalling induces Nox2-dependent IGF-IRβ and/or IRβ transactivation

Intracellular signalling cascades triggered by FPR2 include the activation of several protein kinases, TKRs and PTPases [3,11,14,25,38,43,64]. As a result of FPR2-mediated TKR transactivation, cytosolic phospho-tyrosine residues of TKRs provide docking sites for recruitment and triggering of the STAT3, PLC-γ1/PKCα and PI3K/Akt pathways in different cell lines [11,14].

Since GLUT4 is the insulin-regulated member of glucose transporter family, we analysed the ability of FPR2 to transactivate insulin-like growth factor-I receptor β (IGF-IRβ) and/or insulin receptor β (IRβ). Three tyrosine residues within the

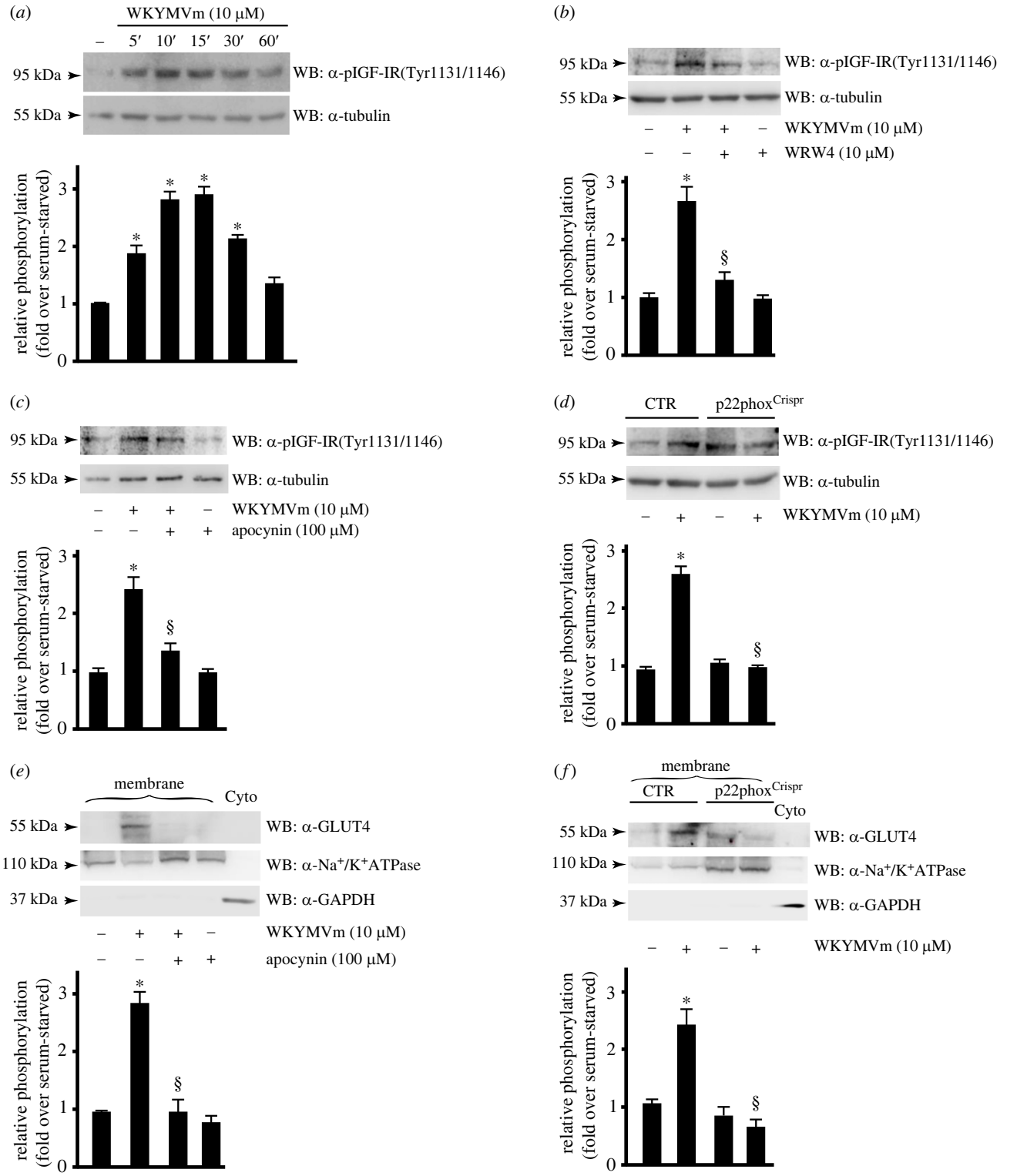

Figure 2. NADPH oxidase-dependent ROS generation modulates FPR2-mediated IGF-IR trans-phosphorylation and GLUT4 membrane translocation. (*a–d*) FPR2-dependent IGF-IR transactivation requires Nox2 activity. (*a*) CaLu-6 cells were growth-arrested for 24 h and stimulated for 5, 10, 15, 30 or 60 min with WKYMVm, or (*b*) pretreated with WRW4, or (*c*) preincubated with apocynin, before stimulation. (*d*) CaLu-6-control$^{Crispr/Cas9}$ cells (CTR) and p22phox$^{Crispr/Cas9}$ (p22phox^{Crispr}) cells were serum-deprived for 24 h and then stimulated with WKYMVm. Fifty micrograms of whole lysates was resolved on 10% SDS-PAGE and incubated with an anti-pIGF-IR(Tyr1131/1146) antibody (α-pIGF-IR(Tyr1131/1146)). An anti-tubulin antibody (α-tubulin) was used as a control for protein loading. (*e*,*f*) GLUT4 membrane translocation depends on ROS generation. Sixty micrograms of membranes lysates was immunoblotted with anti-GLUT4 antibody (α-GLUT4). An anti-Na^+/K^+ATPase antibody (α-Na^+/K^+ATPase) was used as a control for protein loading. Sixty micrograms of a cytosolic proteins (Cyto) was loaded and an anti-GAPDH antibody (α-GAPDH) was used as a control. Data are representative of five independent experiments. *$p < 0.05$ compared to unstimulated cells. §$p < 0.05$ compared to WKYMVm-stimulated cells.

kinase domain (Y1131, Y1135 and Y1136) are the major autophosphorylation sites of IGF-IR*β* [65], which are necessary for kinase activation [66]. IR*β* shares significant structural and functional similarity with IGF-IR*β*, including the presence of an equivalent tyrosine cluster (Y1146, Y1150, Y1151). We used a monoclonal phospho-antibody able to detect both phosphorylated IGF-IR*β* and/or IR*β* and observed that FPR2 stimulation induces time-dependent IGF-IR*β* and/or IR*β* transactivation (figure 2*a*). Pre-treatment with WRW4, before WKYMVm stimulation, prevents IGF-IR*β*/IR*β*

tyrosine phosphorylation (figure 2*b*), thus indicating that it depends on FPR2 activation.

In CaLu-6 cells FPR2 stimulation triggers Nox2 activation [14,25,38] and in several experimental systems the molecular mechanisms responsible for FPR2-dependent TKR trans-phosphorylation require Nox2 activity [11,14]. Therefore, we next preincubated CaLu-6 cells with apocynin, which prevents both $p47^{phox}$ translocation and its interaction with $p22^{phox}$ [67,68], before FPR2 stimulation and we observed that the pretreatment prevents IGF-IRβ/IRβ transactivation (figure 2*c*). By CRISPR/Cas9-based genome editing, we obtained a Calu-6 cell line expressing a non-functional form of $p22^{phox}$ ($p22phox^{Crispr/Cas9}$) [25]. Significantly, stimulation of these cells with WKYMVm failed to induce IGF-IRβ/IRβ phosphorylation (figure 2*d*), showing further evidences that ROS are signalling intermediates in TKR activation [69–72]. Since FPR2-mediated IGF-IRβ/IRβ transactivation depends on Nox2 activity (figure 2*c*,*d*) we investigated the role of Nox2 in GLUT4 membrane translocation. We preincubated Calu-6 cells with the Nox-specific inhibitor apocynin, before WKYMVm stimulation (figure 2*e*) and we incubated $p22phox^{Crispr/Cas9}$ cells with the FPR2 agonist (figure 2*f*). The results show that blockade of Nox2 function prevents FPR2-induced GLUT4 translocation, suggesting that both FPR2-dependent glucose uptake and insulin receptor trans-phosphorylation are modulated by ROS generation.

3.3. FPR2 signalling induces glucose oxidation in the glycolytic pathway

Cancer cells increase glucose uptake and metabolism via glycolysis to meet the bioenergetic demands of rapid cell division [73]. Glycolysis is regulated at several steps via multiple mechanisms but the critical control point is the irreversible reaction catalysed by the 6-phosphofructo-1-kinase (PFK1) enzyme that converts fructose 6-phosphate (F6P) to F1,6BP. In our metabolomic analysis we observed an increase of F1,6BP in FPR2-stimulated cells (figure 1*a*). PFK1 is an allosteric enzyme regulated by fructose-2,6-bisphosphate (F2,6BP), the key activator of glycolysis, and by a variety of other metabolites. Intracellular F2,6BP levels are regulated by the bifunctional 6-phosphofructo-2-kinase/fructose-2,6-bisphosphatase (PFKFB2) enzyme that shows both kinase activity, which converts F6P to F2,6BP, and phosphatase activity, which catalyses the remotion of a phosphate in F2,6BP to generate F6P [74]. PFKFB exists as four isoenzymes (PFKFB1–4), the products of separate genes each with a distinct activity [74–76]. PFKFB2 is mainly expressed in lung, brain and heart [76,77], and its regulation by phosphorylation leads to an increase in F2,6BP concentration and thus to an enhanced glycolysis [78]. In human, the two main activating phosphorylation sites identified in PFKFB2 are Ser^{466} and Ser^{483} residues [78].

We analysed FPR2-induced PFKFB2 phosphorylation by using an anti-phospho specific antibody and observed that either WKYMVm or ANXA1 trigger time-dependent PFKFB2 Ser^{483} phosphorylation (figure 3*a*,*c*), which was completely prevented by preincubation with WRW4 (figure 3*b*,*d*). Notably, the extent of PFKBP2 Ser^{483} phosphorylation appears to be sustained for longer times in cells stimulated with WKYMVm compared to ANXA1. Probably, these differences could be associated with the different nature of the agonists and thier different binding site in FPR2.

Since Ser^{483} residue of PFKFB2 is a target of Akt [78,79], we preincubated cells with wortmannin or LY294002 before WKYMVm stimulation and observed that these treatments prevented FPR2-induced PFKFB2 activation (figure 3*e*).

We analysed the role of other cell surface receptors, besides FPR2, involved on the activation of PI3K/Akt cascade and, in turn, in PFKFB2 Ser^{483} phosphorylation. To this aim we preincubated cells with GSK1904529A, that blocks IGF-IR autophosphorylation and downstream signalling [80], or LY2874455, a potent selective pan-FGFR inhibitor [81], or AG1478, a selective EGFR inhibitor [82], before WKYMVm stimulation. Western blot analysis showed that only FGFR inhibition prevents FPR2-induced PFKFB2 Ser^{483} phosphorylation (figure 3*f*), thus suggesting a cross-talk between FPR2 and FGFR in these cells. FGFR1–4 belong to the FGFR family of TKRs [83,84]. Ligand binding to FGFRs results in phosphorylation at Tyr^{196}, Tyr^{306}, Tyr^{349}, Tyr^{392} and Tyr^{436} residues of the adaptor/scaffold phosphoprotein FGF receptor substrate 2 (FRS2) [85,86] and subsequent activation of PI3K/Akt pathway [87]. In immunoblot experiments we observed that WKYMVm stimulation induced a time-dependent phosphorylation of FRS2 at Tyr^{436} residue (figure 3*g*) which was prevented by the FPR2 antagonist (figure 3*h*).

These results demonstrate that FPR2 signalling directs cells towards the glycolytic pathway by promoting kinase activity of the bifunctional enzyme PFKFB2 through FGFR/FRS2- and Akt-dependent phosphorylation.

3.4. FPR2 signalling prevents the entry of pyruvate in the tricarboxylic acid cycle

PDC is at the centre of aerobic metabolism of carbohydrates. It converts pyruvate into acetyl-CoA and thereby modulates the entry of glucose-derived carbons into the TCA cycle, thus regulating the flow of energy in mammalian cells [88,89]. PDC is composed of three catalytic enzymes and of their respective regulatory proteins [90]. PDC activity is under the control of pyruvate dehydrogenase kinase (PDHK) and pyruvate dehydrogenase phosphatase (PDP), through a reversible phosphorylation–dephosphorylation cycle [91,92]. Pyruvate dehydrogenase is a heterotetrameric enzyme composed of two alpha (PDHA1) and two beta (PDHB1) subunits. PDHA1 is phosphorylated by PDHK1-4 and dephosphorylated by PDP1 and PDP2. The phosphorylation at Ser^{293}, Ser^{300} and Ser^{232} residues on PDHA1 decreases PDC activity and contributes to tumour metabolic reprogramming toward glycolysis in hypoxia, by inhibiting acetyl-CoA formation and the entry in the TCA cycle [91,93–95]. We observed that FPR2 stimulation by WKYMVm or ANXA1 induced a comparable PDHA1 phosphorylation kinetics at Ser^{293} residue (figure 4*a*,*c*) that was prevented by preincubation with WRW4 (figure 4*b*,*d*). Similar results were obtained in A549 lung cancer cell line expressing FPR2 [96] (electronic supplementary material, figure S1).

The PI3K signalling pathway regulates glucose metabolism [97,98] and induces, among other things, Thr^{346} phosphorylation and activation of PDHK1 [99]. Active PDHK1 phosphorylates PDHA1 that, in turn, phosphorylates

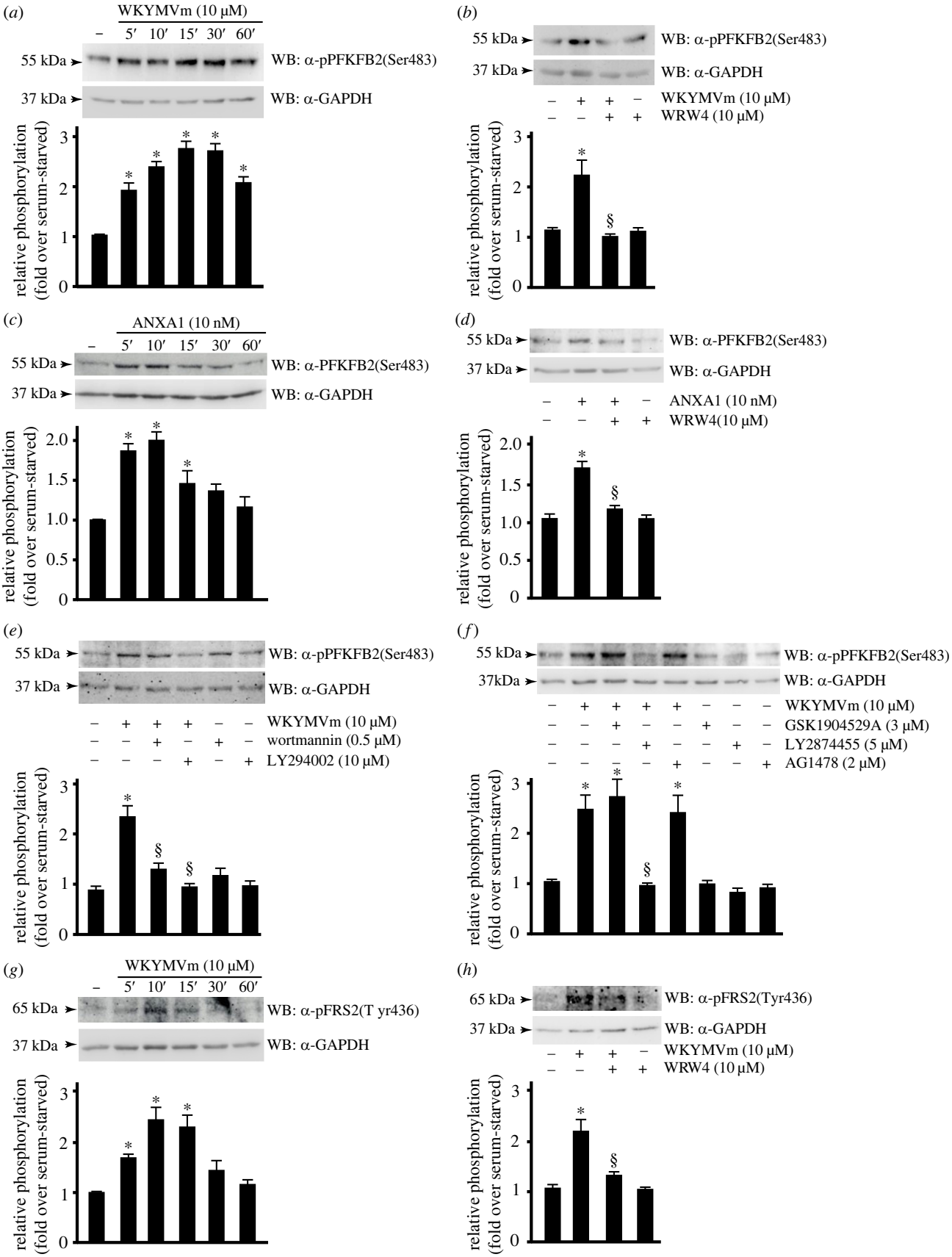

Figure 3. FPR2 signalling triggers FGFR1- and Akt-dependent glucose oxidation. (*a–d*) FPR2 stimulation induces PFKFB2 activation. (*a*) CaLu-6 cells were serum-deprived for 24 h and stimulated for 5, 10, 15, 30 or 60 min with WKYMVm or (*c*) with ANXA1. (*b,d*) Cells were preincubated with WRW4 before stimulation. (*e–h*) PFKFB2 phosphorylation depends on Akt activation and FGFR1 transactivation. (*e*) Cells were stimulated with 10 µM WKYMVm, or preincubated with wortmannin or LY294002, or (*f*) with GSK1904529A or LY2874455 or AG1478, before stimulation. (*g,h*) FPR2 signalling induces the activation of the scaffold phosphoprotein FRS2. (*g*) Serum-starved CaLu-6 cells were stimulated for increased times with WKYMVm as indicated, or (*h*) incubated with the FPR2 antagonist before stimulation. Fifty micrograms of whole lysates was resolved on 10% SDS-PAGE and immunoblotted with (*a–f*) an anti-pPFKFB2(Ser483) antibody (α-pPFKFB2(Ser483)), or with (*g,h*) an anti-pFSR2(Tyr436) antibody (α-pFSR2(Tyr436)). An anti-GAPDH antibody (α-GAPDH) was used as a control for protein loading. Data are representative of four independent experiments. $^{*}p < 0.05$ compared to unstimulated cells. $^{\S}p < 0.05$ compared to WKYMVm-stimulated cells.

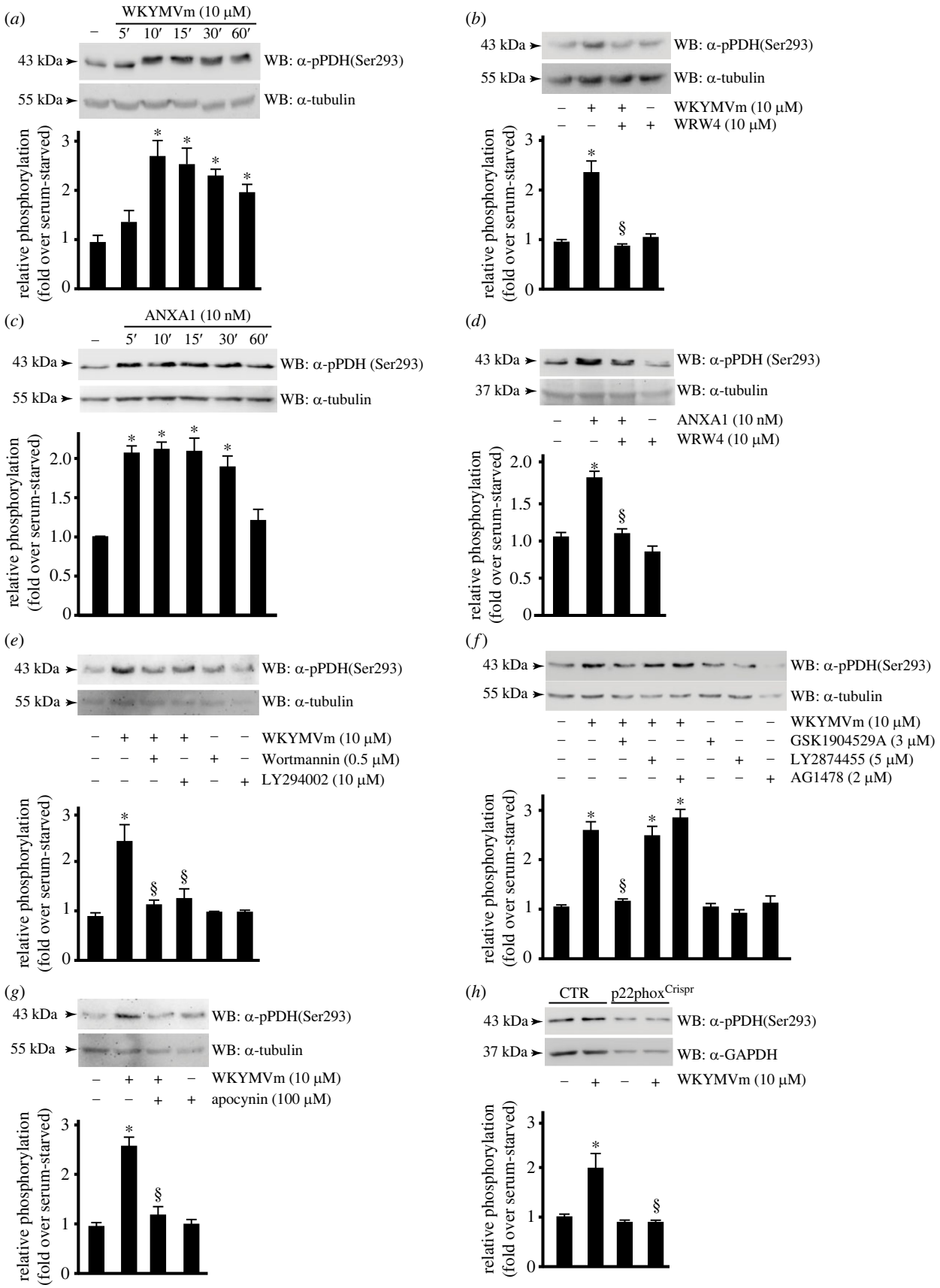

Figure 4. FPR2 signalling prevents pyruvate dehydrogenase activity. (*a*,*c*) FPR2 stimulation induces time-dependent PDH phosphorylation. Serum-deprived CaLu-6 cells were (*a*) stimulated with WKYMVm or (*c*) with ANXA1 for different times. (*b*,*d*) Cells were preincubated with the FPR2 antagonist before stimulation. (*e*) PDH phosphorylation is prevented by PI3K inhibitors. Cells were preincubated with the indicated concentrations of wortmannin or LY294002 before WKYMVm stimulation. (*f*) FPR2-mediated IGF-IR transactivation is required for PDH phosphorylation. Cells were exposed to inhibitors of IGF-IR (GSK1904529A), or FGFR (LY2874455), or EGFR (AG1478) before FPR stimulation. (*g*,*h*) PDH phosphorylation depends on NADPH oxidase activity. (*g*) CaLu-6 cells were preincubated with the indicated concentration of apocynin before stimulation. (*h*) CaLu-6-control$^{Crispr/Cas9}$ cells (CTR) and p22phox$^{Crispr/Cas9}$ (p22phox^{Crispr}) cells were serum-starved for 24 h and then stimulated with WKYMVm. Fifty micrograms of whole lysates was resolved on 10% SDS-PAGE and hybridized with an anti-pPDH(Ser293) antibody (α-pPDH(Ser293)). An anti-GAPDH antibody (α-GAPDH) was used as a control for protein loading. Data are representative of three independent experiments. *$p < 0.05$ compared to unstimulated cells. §$p < 0.05$ compared to WKYMVm-stimulated cells.

and inactivates PDC. We preincubated cells with wortmannin or LY294002, before WKYMVm stimulation, and observed that this treatment prevents FPR2-induced PDHA1 phosphorylation at Ser^{293} residue (figure 4*e*). Binding of insulin, growth factors, and cytokines to cell surface receptors also triggers PI3K activation. We preincubated cells with specific inhibitors of IGF-IRβ/IRβ, FGFR and EGFR and in western blot analysis we observed that only GSK1904529A prevented FPR2-induced PDHA1 Ser^{293} phosphorylation (figure 4*f*), strongly suggesting that it depended on the activation of insulin receptors.

FPRs and activated growth factor receptors increase intracellular ROS generation by activating Nox enzymes or by increasing Nox expression [100,101]. Notably, ROS also modulates Akt activation and MAPK signalling pathways, as well as the activity of several redox-sensitive transcription factors [102,103]. We analysed the role of Nox in PDHA1 regulation and observed that FPR2-induced PDHA1 Ser293 phosphorylation was prevented upon preincubation of cells with the Nox-specific inhibitor apocynin (figure 4*g*) and in the p22phox $^{Crispr/Cas9}$ cells (figure 4*h*) stimulated with WKYMVm.

These results prove that FPR2 signalling induces IGF-IRβ/IRβ-, PI3K/Akt- and Nox-dependent inhibition of PDC and, in turn, promotes the aerobic glycolysis pathway for energy production.

3.5. WKYMVm stimulation actives lactate dehydrogenase A and enhances lactate production

Lactate dehydrogenase A (LDH-A) catalyses lactate formation from pyruvate and ensures the regeneration of NAD^+, which is needed as an electron acceptor in glycolysis [104]. In several human cancer cells LDH-A is activated by phosphorylation at Tyr^{10} residue, which correlates with activation of multiple oncogenic tyrosine kinases commonly increased in cancer [105]. By western blot experiments we showed that FPR2 signalling triggered by WKYMVm or ANXA1 induced time-dependent Tyr^{10} LDH-A phosphorylation (figure 5*a*,*c*), that was prevented by the FPR2 antagonist (figure 5*b*,*d*). Similar results were obtained in A549 lung cancer cell line (electronic supplementary material, figure S2).

The oncogenic receptor tyrosine kinase FGFR1 directly phosphorylates LDH-A at Tyr^{10} residue, thus promoting the formation of an active, tetrameric LDH-A complex [105,106]. Since we proved that FPR2 stimulation induces FGFR transactivation (figure 3*d*), we analysed the role of this oncogenic receptor in LDH-A activation and, by immunoblot experiments, we observed that WKYMVm-induced LDH-A phosphorylation at Tyr^{10} residue was prevented by preincubation with the pan-FGFR inhibitor LY2874455 (figure 5*e*). However, other oncogenic tyrosine kinases, such as Src, phosphorylate LDH-A at Tyr^{10} residue [107]. Therefore, we preincubated cells with PP2, an ATP-competitive inhibitor of the Src protein tyrosine kinases family, or with PP3, a negative control for the Src kinase inhibitor PP2, and we observed that Src inhibition prevents LDH-A phosphorylation at Tyr^{10} residue (figure 5*f*). Src can be recruited to active FGFR1 through the adaptor protein FRS2 at the plasma membrane [108,109]. Since Src activity is regulated by phosphorylation on Tyr^{416} residue in the kinase domain, we analysed Src phosphorylation levels in WKYMVm-stimulated cells preincubated or not with the pan-FGFR inhibitor. By western blot analysis with a phospho-specific antibody we observed that LY2874455 prevents Tyr^{416} phosphorylation of Src (figure 5*g*). Furthermore, in line with the FPR2-dependent LDH-A activation, we found that this correlates with an FPR2-dependent increased production of lactate (figure 5*h*). Taken together these results show that in CaLu-6 cells FPR2 signalling triggers FGFR1- and Src-dependent LDH-A activation, thereby promoting lactate production in CaLu-6 cells.

3.6. FPR2 stimulation induces HIF-1 and c-Myc activation

LDH-A expression is regulated by c-Myc and hypoxia inducible factor-1 (HIF-1) [110]. These two transcriptional factors cooperate to induce a transcriptional programme for hypoxic adaptation [111], as well as to improve the metabolic needs of cancer cells, by increasing glucose absorption and its conversion to lactate. Hypoxic signalling pathways are implicated in a plethora of physiological processes and they are centrally involved in hyperproliferative disease processes [112]. The central axis of hypoxic signalling is the activation of HIF-1, which consists of an oxygen-regulated HIF-1α subunit and a constitutively expressed HIF-1β subunit. Under normoxic conditions, HIF-1α is hydroxylated on two proline residues by prolyl hydroxylases, leading to its rapid proteasomal degradation. By contrast, hypoxic conditions inhibit HIF-1α degradation leading to its stabilization and nuclear translocation [113]. In the nucleus, HIF-1α dimerizes with HIF-1β and binds to cis-acting hypoxia response elements (HREs) in several target genes, including those involved in glucose uptake, glycolytic enzyme synthesis, lactate generation and secretion [114]. Therefore, we first evaluated the ability of FPR2 to induce HIF-1α stabilization and, in immunoblot experiments performed on whole protein extracts of CaLu-6 cells, we observed a time-dependent accumulation of this protein (figure 6*a*), which was prevented by WRW4 (figure 6*b*). Nox-dependent ROS generation is involved in hypoxic signalling in primary lung cells and, in turn, in HIF-1α stabilization [112]. In agreement, we observed that Nox inhibition by apocynin (figure 6*c*) or by CRISPR/Cas9-based $p22^{phox}$ editing (figure 6*d*) prevents HIF-1α accumulation in FPR2-stimulated CaLu-6 cells.

FPR2 localizes also in nuclear fractions of CaLu-6 and AGS cells and nuclear FPR2 activation prompts a decreased Gαi-FPR2 association and triggers ERKs, c-Jun and c-Myc activation [26]. In response to a growth-stimulatory signal, c-Myc protein is phosphorylated at Ser^{62} residue, which results in its stabilization [115]. Interestingly, by western blot analysis performed in WKYMVm-stimulated CaLu-6 cells with an anti-Myc(pSer62) antibody, we detected a time-dependent increase of Myc phosphorylation (figure 6*e*), which was prevented by FPR2 antagonist pretreatment (figure 6*f*).

These results demonstrate that FPR2 signalling controls HIF-1 and c-Myc activation, which are involved in the transcriptional regulation of genes involved in the metabolism of glucose.

3.7. FPR2 stimulation improves energetic metabolism of CaLu-6 cells

We further evaluated the effect of FPR2 stimulation on glucose metabolism in lung cancer CaLu-6 cells by using

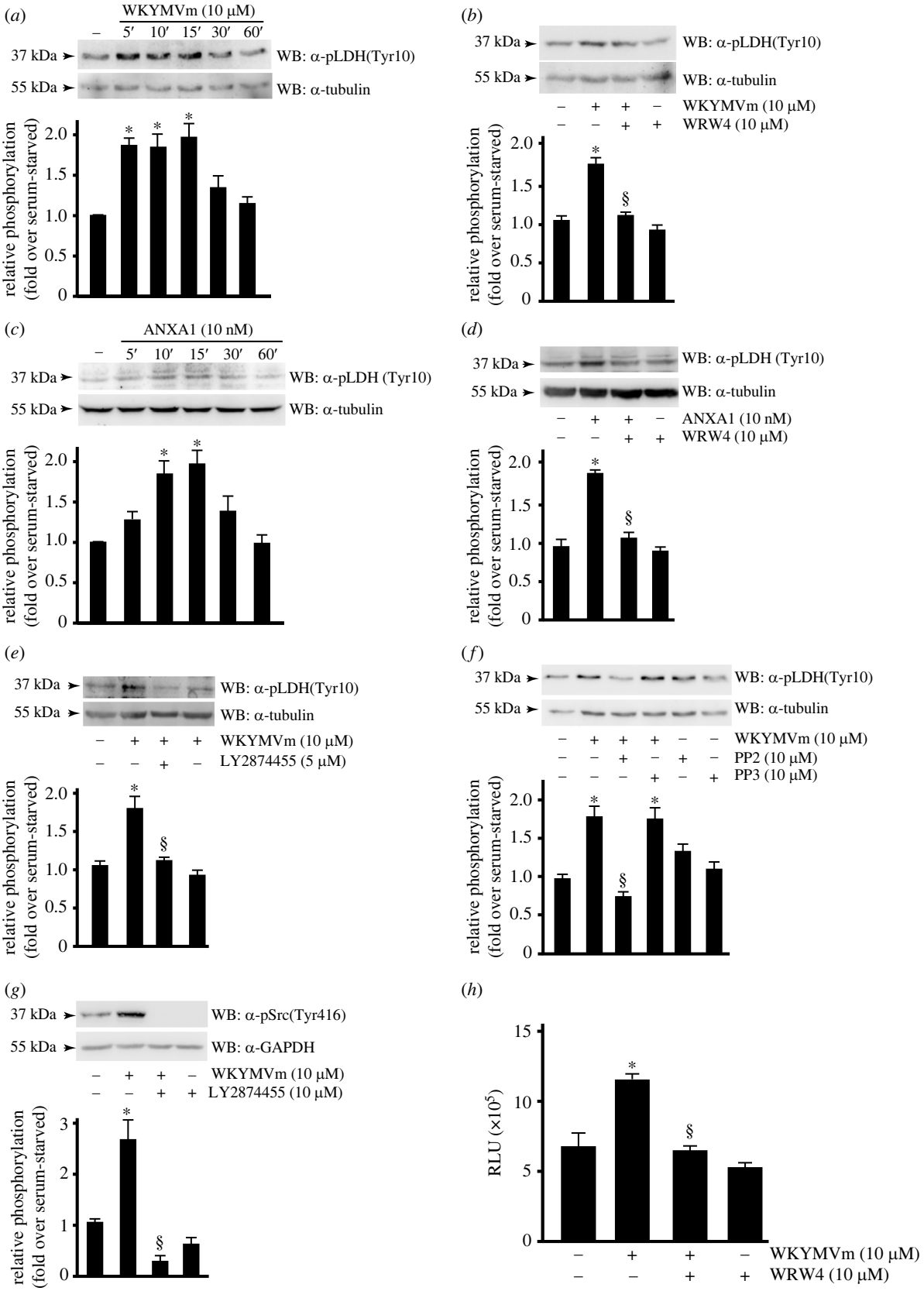

Figure 5. FPR2 stimulation induces LDH activity and an enhanced production of lactate. (*a–d*) FPR2 stimulation induces time-dependent LDH phosphorylation. Growth-arrested CaLu-6 cells were stimulated with (*a*) WKYMVm or (*c*) ANXA1 for 5, 10, 15, 30 or 60 min, or (*b*,*d*) preincubated with WRW4. (*e*) LDH activity depends on FPR2-dependent FGFR1 transactivation. Serum-starved cells were preincubated with the FGFR pan-inhibitor LY2874455, at the indicated concentration, before WKYMVm stimulation. (*e–g*) FGFR1-recruited Src phosphorylates LDH. (*f*) Cells were preincubated with PP2 or PP3, or (*e*,*g*) with LY2874455, at the indicated concentrations before stimulation. Fifty micrograms of whole lysates was resolved on 10% SDS-PAGE and incubated with (*a–f*) an anti-pLDH(Tyr10) antibody (α-pLDH(Tyr10)), or with (*g*) anti-pSrc(Tyr416) (α-pSrc(Tyr416)). An anti-GAPDH antibody (α-GAPDH) was used as a control for protein loading. Data are representative of five independent experiments. (*h*) Representative bar graphs of lactate concentration measured in cell culture media. CaLu-6 cells were serum-starved for 24 h, preincubated with WRW4 and then stimulated with WKYMVm. The media from cell cultures were collected and lactate concentration was measured by using a commercial kit following manufacturer's instructions. Results are the mean of three independent experiments and in each separated experiment every point was analysed in triplicate. $^{*}p < 0.05$ compared to unstimulated cells. $^{\S}p < 0.05$ compared to WKYMVm-stimulated cells.

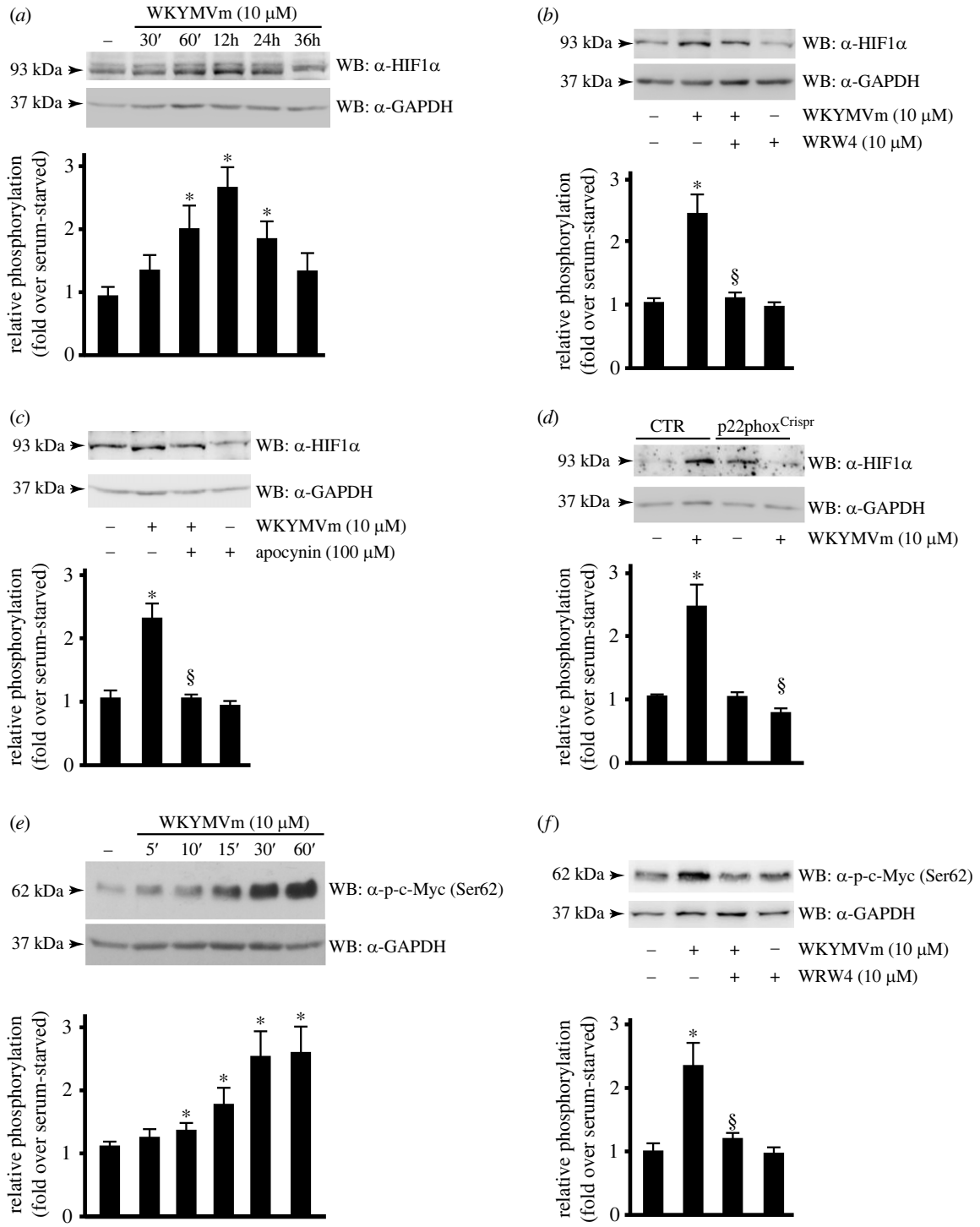

Figure 6. FPR2 activation by WKYMVm induces Nox-dependent HIF-1α stabilization and c-Myc phosphorylation. (*a*,*b*) FPR2 signalling triggers time-dependent accumulation of HIF-1α. (*a*) Serum-starved CaLu-6 cells were stimulated with WKYMVm for the indicated times, or (*b*) preincubated with WRW4 before stimulation. (*c*,*d*) FPR2-dependent HIF-1α stabilization requires Nox2 activity. (*c*) Cells were preincubated with apocynin, before exposure to WKYMVm. (*d*) CaLu-6-control$^{Crispr/Cas9}$ cells (CTR) and p22phox$^{Crispr/Cas9}$ (p22phox^{Crispr}) cells were serum-starved for 24 h and then stimulated for 12 h with WKYMVm. (e,*f*) FPR2 signalling triggers time-dependent c-Myc phosphorylation. (*e*) Cells were incubated for increased times with the FPR2 agonist, as indicated, or (*f*) exposed to WRW4 before stimulation. Fifty micrograms of whole lysates was electrophoresed on 10% SDS-PAGE and incubated with (*a–d*) an anti-HIF1α antibody (α-HIF1α), or (*e*,*f*) with an anti-p-c-Myc(Ser62) (α-p-c-Myc(Ser62)). An anti-GAPDH antibody (α-GAPDH) was used as a control for protein loading. Western blot data are representative of five independent experiments. *$p < 0.05$ compared to unstimulated cells. $^{§}p < 0.05$ compared to WKYMVm-stimulated cells.

Seahorse XF glycolytic rate assay. This assay provides accurate measurements of glycolytic rates for basal conditions and compensatory glycolysis following mitochondrial inhibition. The calculated rates account for contribution of CO_2 to extracellular acidification derived from mitochondrial/TCA cycle activity and are directly comparable to lactate accumulation data. Firstly, we measured the real time extracellular acidification rate (ECAR) in serum-starved cells stimulated or not with WKYMVm for 24 h. Kinetic data showed a significant increase of the ECAR in FPR2-stimulated cells (figure 7*a*). In addition, the proton efflux rate (PER) value provides a more accurate measurement of extracellular acidification (pmol H^+ min^{-1}), by calculating the total proton efflux derived from glycolytic and mitochondrial

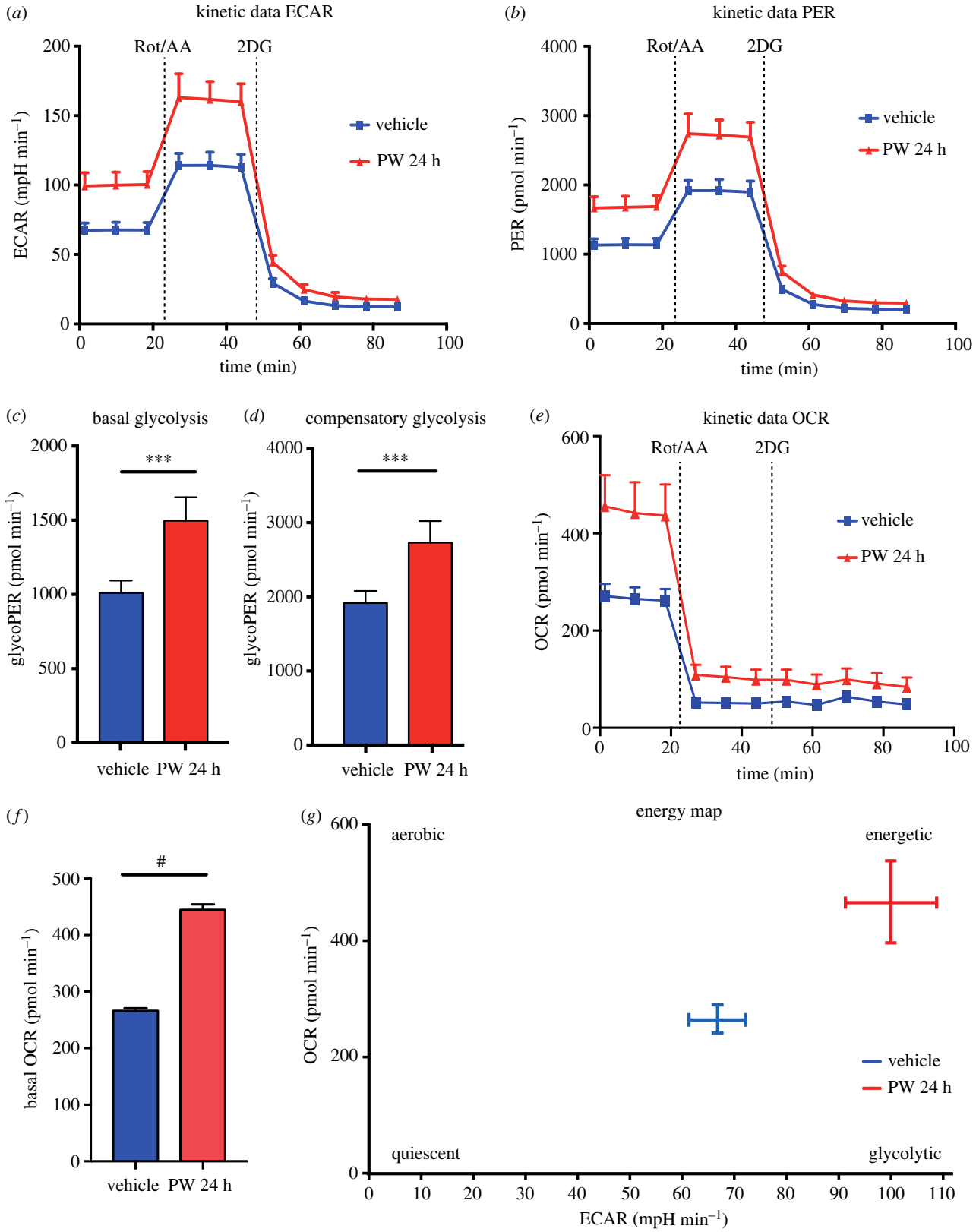

Figure 7. Seahorse analysis of WKYMVm-stimulated CaLu-6 cells. Extracellular acidification rate (ECAR) (*a*) and proton efflux rate (PER) (*b*) were measured in Calu-6 cells treated for 24 h with 10 µM WKYMVm (red line) or vehicle (blue line). Basal ECAR and PER measurements were followed by sequential treatment (dotted vertical lines) with rotenone plus antimycin A (Rot/AA) and 2-deoxyglucose (2DG). Bar graphs represent (*c*) basal and (*d*) compensatory PER produced from glycolysis (glycoPER). (*e*,*f*) Basal oxygen consumption rate (OCR) was measured in Calu-6 cells treated with 10 µM WKYMVm (red line) or vehicle (blue line) for 24 h. (*g*) Metabolic profile of CaLu-6 cells exposed to 10 µM WKYMVm (red) or vehicle (blue) for 24 h. ***$p < 0.001$ and ****$p < 0.0001$ compared to unstimulated cells.

acidification. Consistent with ECAR, PER was significantly enhanced upon WKYMVm exposure in CaLu-6 cells compared to unstimulated cells (figure 7*b*). Furthermore, inhibition of mitochondrial respiration by rotenone and antimycin A (Rot/AA) was used to calculate the glycolytic proton efflux rate (glycoPER), thus estimating the proton efflux derived from glycolysis. Our results showed that FPR2 stimulation, measured after blockade of mitochondrial electron transport chain, significantly upregulated glycoPER in both basal (figure 7*c*) and compensatory glycolysis

(figure 7*d*). In addition, WKYMVm stimulation significantly increased mitochondrial basal respiration compared to untreated CaLu-6 cells, as suggested by oxygen consumption rate (OCR) measurement (figure 7*e,f*). Previously we demonstrated that FPR2 stimulation significantly improves the expression of the glutamine transporter ASCT2, which correlates with an increase of glutamine uptake [45]. Glutaminase converts glutamine in glutamate that is transaminated in alpha-ketoglutarate. This fuels the TCA to generate ATP and citrate contributing to mitochondrial respiration and thus to an increase of OCR. Notably, FPR2-stimulated cells showed significant changes in both OCR and ECAR compared to unstimulated cells, suggesting a switch towards a more energetic phenotype (figure 7*g*).

Taken together, these data clearly demonstrate that FPR2 stimulation enhances energetic metabolism of Calu-6 cells.

4. Discussion

By using a metabolomic approach, we have analysed metabolic pathways activated in FPR2-stimulated CaLu-6 cells, a human lung cancer cell line. Metabolic data reveal that FPR2 stimulation increases cellular concentration of metabolites involved in glucose metabolism, such as glucose 6P, F1,6BP, GA3P and lactate. We prove that FPR2 stimulation enhances glucose uptake in a time-dependent manner by increasing GLUT4 cellular membrane localization through insulin receptor-dependent PI3K/Akt signalling cascade. FPR1 stimulation, another member of the FPR family expressed in a range of tissues and cell types [116], also enhances glucose uptake and GLUT4 translocation via Akt activation [117]. Furthermore, the FPR1 agonist formyl-methionyl-leucyl-phenilalanine (fMLP) peptide induces GLUT1 and GLUT5 membrane translocation in human monocytes [118] and stimulates 2-deoxyglucose uptake in macrophage in association with an increase of GLUT3 on the membrane [119]. GLUT4 is the insulin-regulated member of transmembrane glucose transporter family and consistently we show that WKYMVm stimulation triggers FPR2- and Nox2-dependent IGF-IRβ/IRβ trans-phosphorylation. GPCRs and TKRs are not to be only considered as distinct signalling units; indeed GPCR-mediated TKR transactivation is a proven molecular mechanism able to increase the number and range of cellular signalling networks. IGF-IR is transactivated by $GABA_B$, thrombin, metabotropic glutamate, neurotensin and angiotensin II (AngII) type receptors [120–124]. In this paper, we provide the first demonstration that FPR2 functionally transactivates IGF-IR in a human cancer cell line.

We prove that FPR2 signalling directs cells towards the glycolytic pathway by promoting Akt- and FGFR-dependent kinase activity of the bifunctional enzyme PFKFB2. Several GPCRs form heterocomplexes with FGFRs and control the cell fate [125–133]. Our data reveal for the first time in epithelial cancer cells a cross talk between FPR2 and FGFR1, as well as the activation of the scaffold phosphoprotein FSR2, which acts as a docking protein downstream to phosphorylated FGFR1.

Pyruvate arising from glycolysis can be converted in acetyl-CoA by an oxidative decarboxylation catalysed by PDH, or in lactate by an oxidoreduction reaction catalysed by LDH. In cancer cells the production of lactate and H^+ ions plays crucial roles in: (i) synthesis of NAD^+ necessary to sustain the increased rate of glycolysis; (ii) acidification of the tumour microenvironment, thus reducing the viability of normal cells and favouring the infiltration of neoplastic cells [134]; and (iii) binding to specific receptors on target cells, such as GPR81, thus activating intracellular signalling cascades, lactate uptake, mitochondrial metabolism, angiogenesis and tumour growth [135–137]. We demonstrate that FPR2 signalling triggers PDHK1-mediated PDHA1 phosphorylation at Ser^{293}. Therefore, by suppressing the oxidative decarboxylation of pyruvate, phosphorylated PDHK1 shuts off oxidative phosphorylation, maintains tumour cell proliferation in severe hypoxia conditions, and switches cancer metabolism towards glycolysis. We also reveal an increase of LDH-A activity that is involved in lactate production and that significantly contributes to the Warburg effect [138,139]. Cancer cells reprogramme their metabolism to support survival, growth and proliferation, and they synthesize large amounts of lactate independently of the oxygen availability. Since the oxidation of glucose to lactate generates 2 ATPs per molecule of glucose, whereas oxidation of pyruvate in TCA and oxidative phosphorylation generate up to 36 ATPs, the Warburg effect has been proposed as a mechanism to support the biosynthetic requirements of cancer cells. In fact, carbon atoms derived from the increased glucose consumption can be used for anabolic processes needed to support cell proliferation, such as de novo synthesis of nucleotides, lipids, and proteins [140–143]. This implies that cancer cells are in greater need of reducing equivalents in the form of NADPH, which is necessary for reductive biosynthesis. Increased glucose uptake allows an enhanced synthesis of NADPH in the oxidative branch of PPP which also provides ribose-5P for the synthesis of nucleotides. Accordingly, in our metabolomic analysis we observed an increase of NADPH production via PPP and the activation of the multifunctional enzyme CAD that participates in the three initial speed-limiting steps of the de novo synthesis of pyrimidine nucleotides in mammals [45]. The regeneration of NAD^+ from NADH in the reaction catalysed by LDH represents another mechanism that accounts for the biosynthetic function of the Warburg effect. In this scenario NADH is consumed to regenerate NAD^+, to keep glycolysis active in cancer cells and to allow the biosynthesis of serine from 3-phosphoglycerate. Serine is required for many biosynthetic and signalling pathways and provides a carbon unit into the folate-dependent biosynthesis of purine nucleotides [144].

We prove that FPR2 signalling induces HIF-1 stabilization and c-Myc activation. Interestingly, these two transcriptional factors cooperate to regulate LDH-A expression and to activate hexokinase 2 and PDK1, resulting in enhanced conversion of glucose to lactate [145]. HIF-1 is also a determinant for GLUT4-mediated glucose uptake [146].

Nox2-dependent ROS generation plays also a crucial role in the molecular mechanisms that we herein describe. In fact, we show that ROS cellular levels regulate (i) GLUT4 membrane localization; (ii) FPR2-mediated IGF-IRβ/IRβ transactivation; (iii) PDH phosphorylation; and (iv) HIF1α stabilization. Accordingly, in skeletal muscle fibres, Nox2 regulates glucose transport capacity through GLUT4 and AngII-mediated IGF-1R transactivation [147,148]. Furthermore, some evidence suggests that ROS inhibition prevents PDH phosphorylation [149] and that ROS may activate PDKs [150]. Nox-derived ROS can also enhance HIF activation [151,152]. In fact, the increase in ROS generation observed in cells overexpressing Nox1 is associated with the

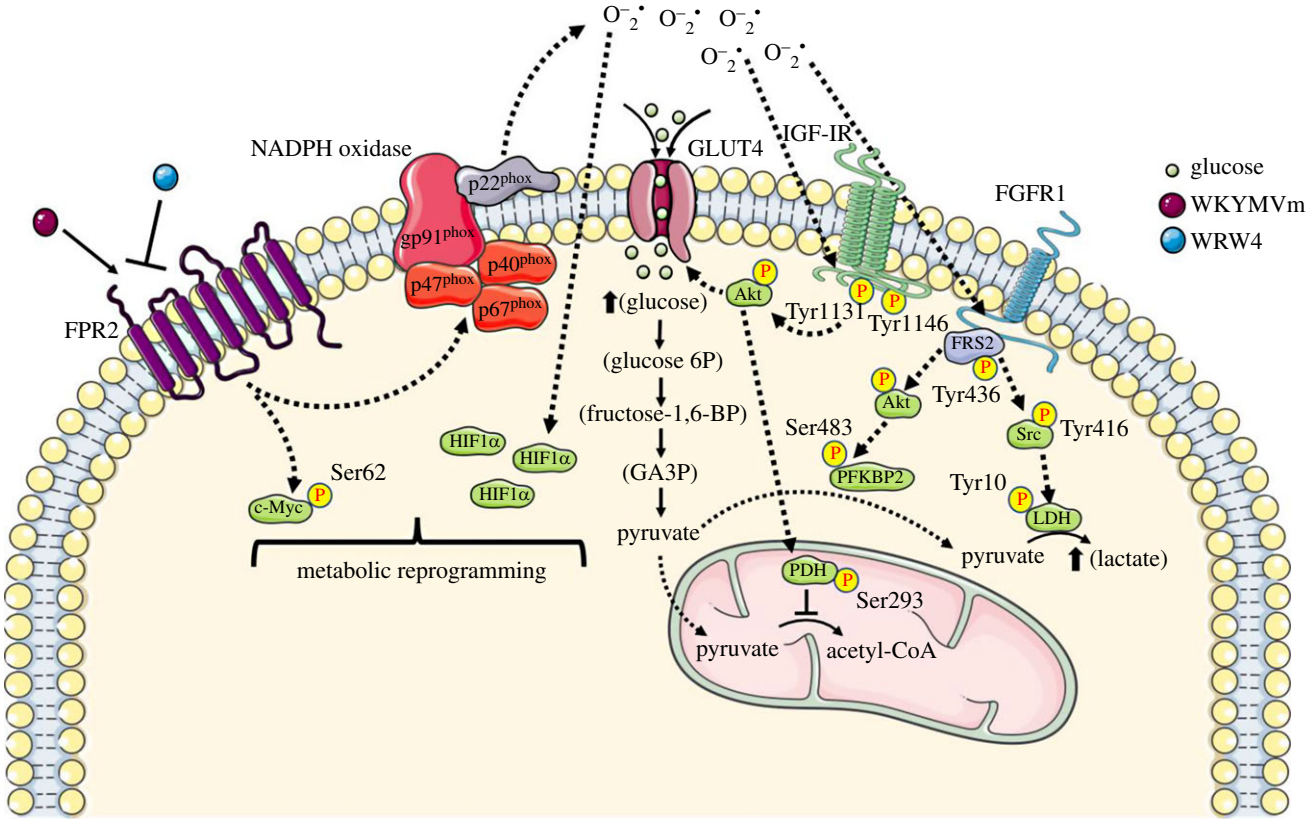

Figure 8. Integration between signalling pathways triggered by FPR2 and glucose metabolism. FPR2 stimulation by WKYMVm induces NADPH oxidase-dependent ROS generation, which is involved in IGF-IR and FGFR transactivation. IGF-IR stimulates cellular glucose uptake by inducing Akt-dependent translocation of GLUT4 to the plasma membranes. FPR2 signalling directs glucose towards the glycolytic pathway by promoting kinase activity of the bifunctional enzyme PFKFB2 through FGFR/FRS2/Akt-dependent phosphorylation. Intracellular pathways triggered by FPR2 also induce IGF-IR/Akt-dependent inhibition of PDH and, in turn, promote aerobic glycolysis pathway for energy production. Src, activated by FGFR/FRS2 cascade, phosphorylates LDH with the consequent enhanced production of lactate. ROS induce Nox-dependent HIF-1α stabilization and c-Myc phosphorylation which cooperate to regulate LDH expression.

activation of HIF-1-dependent target gene expression [153], and Nox4 activation by thrombin increases HIF-2α protein levels [154]. Interestingly, Nox4 is a transcriptional target of HIF-1α [155]. However, further studies in models of lung cancer should be performed in order to extend the knowledge on the role of FPR2 in metabolic reprogramming.

5. Conclusion

The emerging view of metabolic regulation in cancer cells is that signal transduction networks participate in a substantial reorganization of metabolic activities. Since Warburg's early observations, much information on glucose metabolism in cancer cells has been understood, but the integration between signalling pathways and cellular metabolism is still unclear. This study provides new insights into the molecular mechanisms by which FPR2-induced/TKR signalling and Nox2-dependent ROS generation regulate glucose metabolism in CaLu-6 cancer cells. FPR2 stimulation triggers intracellular signalling cascades that induce TKR transactivation, insulin-dependent glucose uptake, the activation of regulatory glycolytic enzymes, the promotion of aerobic glycolysis for energy production, instead of mitochondrial oxidative phosphorylation, and both an enhanced LDH activity and lactate production (figure 8). Therefore, FPR2 signalling and Nox2 regulatory subunits are promising therapeutic targets to be explored for the treatment of human cancers.

Ethics. This work did not require ethical approval from a human subject or animal welfare committee.

Data accessibility. The data are provided in electronic supplementary material [156].

Declaration of AI use. We have not used AI-assisted technologies in creating this article.

Authors' contributions. T.P.C.: formal analysis, investigation; E.P.: conceptualization, formal analysis, investigation; M.S.: data curation, formal analysis, methodology; G.E.: writing—original draft; R.A.: data curation, validation, writing—original draft, writing—review and editing; F.C.: conceptualization, funding acquisition, project administration, supervision, validation, writing—original draft, writing—review and editing.

All authors gave final approval for publication and agreed to be held accountable for the work performed therein.

Conflict of interest declaration. We declare we have no competing interests.

Funding. This work was funded by Universita' degli Studi di Napoli, Italy, Finanziamento Ricerca di Ateneo 2020 (2020 SDPFOSAA).

References

1. Hilger D, Masureel M, Kobilka BK. 2018 Structure and dynamics of GPCR signaling complexes. *Nat. Struct. Mol. Biol.* **25**, 4–12. (doi:10.1038/s41594-017-0011-7)

2. Cabrera-Vera TM, Vanhauwe J, Thomas TO, Medkova M, Preininger A, Mazzoni MR, Hamm HE. 2003

Insights into G protein structure, function, and regulation. *Endocr. Rev.* **24**, 765–781. (doi:10.1210/er.2000-0026)

3. Cattaneo F, Guerra G, Parisi M, De Marinis M, Tafuri D, Cinelli M, Ammendola R. 2014 Cell-surface receptors transactivation mediated by g protein-coupled receptors. *Int. J. Mol. Sci.* **15**, 19 700–19 728. (doi:10.3390/ijms151119700)
4. Grisanti LA, Guo S, Tilley DG. 2017 Cardiac GPCR-mediated EGFR transactivation: impact and therapeutic implications. *J. Cardiovasc. Pharmacol.* **70**, 3–9. (doi:10.1097/FJC.0000000000000462)
5. Crudden C, Shibano T, Song D, Suleymanova N, Girnita A, Girnita L. 2018 Blurring boundaries: receptor tyrosine kinases as functional G protein-coupled receptors. *Int. Rev. Cell Mol. Biol.* **339**, 1–40. (doi:10.1016/bs.ircmb.2018.02.006)
6. Kilpatrick LE, Hill SJ. 2021 Transactivation of G protein-coupled receptors (GPCRs) and receptor tyrosine kinases (RTKs): recent insights using luminescence and fluorescence technologies. *Curr. Opin. Endo. Metab. Res.* **16**, 102–112. (doi:10.1016/j.coemr.2020.10.003)
7. Schroder K. 2019 NADPH oxidase-derived reactive oxygen species: Dosis facit venenum. *Exp. Physiol.* **104**, 447–452. (doi:10.1113/EP087125)
8. Kleniewska P, Piechota A, Skibska B, Goraca A. 2012 The NADPH oxidase family and its inhibitors. *Archivum Immunologiae et Therapiae Experimentalis* **60**, 277–294. (doi:10.1007/s00005-012-0176-z)
9. Castaldo M, Zollo C, Esposito G, Ammendola R, Cattaneo F. 2019 NOX2-dependent reactive oxygen species regulate formyl-peptide receptor 1-mediated TrkA transactivation in SH-SY5Y Cells. *Oxidative Med. Cell. Longev.* **2019**, 2051235. (doi:10.1155/2019/2051235)
10. Cattaneo F, Castaldo M, Parisi M, Faraonio R, Esposito G, Ammendola R. 2018 Formyl peptide Receptor 1 modulates endothelial cell functions by NADPH oxidase-dependent VEGFR2 transactivation. *Oxidative Med. Cell. Longev.* **2018**, 2609847. (doi:10.1155/2018/2609847)
11. Cattaneo F, Parisi M, Ammendola R. 2013 WKYMVm-induced cross-talk between FPR2 and HGF receptor in human prostate epithelial cell line PNT1A. *FEBS Lett.* **587**, 1536–1542. (doi:10.1016/j.febslet.2013.03.036)
12. Iaccio A, Cattaneo F, Mauro M, Ammendola R. 2009 FPRL1-mediated induction of superoxide in LL-37-stimulated IMR90 human fibroblast. *Arch. Biochem. Biophys.* **481**, 94–100. (doi:10.1016/j.abb.2008.10.026)
13. Ammendola R, Russo L, De Felice C, Esposito F, Russo T, Cimino F. 2004 Low-affinity receptor-mediated induction of superoxide by N-formyl-methionyl-leucyl-phenylalanine and WKYMVm in IMR90 human fibroblasts. *Free Rad. Biol. Med.* **36**, 189–200. (doi:10.1016/j.freeradbiomed.2003.10.015)
14. Cattaneo F, Iaccio A, Guerra G, Montagnani S, Ammendola R. 2011 NADPH-oxidase-dependent reactive oxygen species mediate EGFR transactivation by FPRL1 in WKYMVm-stimulated human lung cancer cells. *Free Rad. Biol. Med.* **51**, 1126–1136. (doi:10.1016/j.freeradbiomed.2011.05.040)
15. Petry A, Weitnauer M, Gorlach A. 2010 Receptor activation of NADPH oxidases. *Antioxid. Redox Signal.* **13**, 467–487. (doi:10.1089/ars.2009.3026)
16. Moloney JN, Cotter TG. 2018 ROS signalling in the biology of cancer. *Semin. Cell Dev. Biol.* **80**, 50–64. (doi:10.1016/j.semcdb.2017.05.023)
17. Wang N *et al.* 2019 Loss of Scribble confers cisplatin resistance during NSCLC chemotherapy via Nox2/ROS and Nrf2/PD-L1 signaling. *EBioMedicine.* **47**, 65–77. (doi:10.1016/j.ebiom.2019.08.057)
18. Yang WH, Huang Z, Wu J, Ding CC, Murphy SK, Chi JT. 2020 A TAZ-ANGPTL4-NOX2 axis regulates ferroptotic cell death and chemoresistance in epithelial ovarian cancer. *Mol. Cancer Res.* **18**, 79–90. (doi:10.1158/1541-7786.MCR-19-0691)
19. Rao Malla R, Raghu H, Rao JS. 2010 Regulation of NADPH oxidase (Nox2) by lipid rafts in breast carcinoma cells. *Int. J. Oncol.* **37**, 1483–1493.
20. Kim YM, Muthuramalingam K, Cho M. 2020 Redox regulation of NOX isoforms on FAK((Y397))/SRC((Y416)) phosphorylation driven epithelial-to-mesenchymal transition in malignant cervical epithelial cells. *Cells* **9**, 1555. (doi:10.3390/cells9061555)
21. Deep G *et al.* 2016 Graviola inhibits hypoxia-induced NADPH oxidase activity in prostate cancer cells reducing their proliferation and clonogenicity. *Sci. Rep.* **6**, 23135. (doi:10.1038/srep23135)
22. Hernandez-Garcia D, Wood CD, Castro-Obregon S, Covarrubias L. 2010 Reactive oxygen species: a radical role in development? *Free Rad. Biol. Med.* **49**, 130–143. (doi:10.1016/j.freeradbiomed.2010.03.020)
23. Barford D. 2004 The role of cysteine residues as redox-sensitive regulatory switches. *Curr. Opin. Struct. Biol.* **14**, 679–686. (doi:10.1016/j.sbi.2004.09.012)
24. Perretti M, Godson C. 2020 Formyl peptide receptor type 2 agonists to kick-start resolution pharmacology. *Br. J. Pharmacol.* **177**, 4595–4600. (doi:10.1111/bph.15212)
25. Ammendola R, Parisi M, Esposito G, Cattaneo F. 2021 Pro-resolving FPR2 agonists regulate NADPH oxidase-dependent phosphorylation of HSP27, OSR1, and MARCKS and activation of the respective upstream kinases. *Antioxidants* **10**, 134. (doi:10.3390/antiox10010134)
26. Cattaneo F, Parisi M, Fioretti T, Sarnataro D, Esposito G, Ammendola R. 2016 Nuclear localization of formyl-peptide receptor 2 in human cancer cells. *Arch. Biochem. Biophys.* **603**, 10–19. (doi:10.1016/j.abb.2016.05.006)
27. He HQ, Ye RD. 2017 The formyl peptide receptors: diversity of ligands and mechanism for recognition. *Molecules* **22**, 455. (doi:10.3390/molecules22030455)
28. Dalli J, Consalvo AP, Ray V, Di Filippo C, D'Amico M, Mehta N, Perretti M. 2013 Proresolving and tissue-protective actions of annexin A1-based cleavage-resistant peptides are mediated by formyl peptide receptor 2/lipoxin A4 receptor. *J. Immunol.* **190**, 6478–6487. (doi:10.4049/jimmunol.1203000)
29. Cooray SN, Gobbetti T, Montero-Melendez T, Mcarthur S, Thompson D, Clark AJL, Flower RJ, Perretti M. 2013 Ligand-specific conformational change of the G-protein-coupled receptor ALX/FPR2 determines proresolving functional responses. *Proc. Natl Acad. Sci. USA* **110**, 18 232–18 237. (doi:10.1073/pnas.1308253110)
30. Kim YE, Park WS, Ahn SY, Sung DK, Sung SI, Kim JH, Chang YS. 2019 WKYMVm hexapeptide, a strong formyl peptide receptor 2 agonist, attenuates hyperoxia-induced lung injuries in newborn mice. *Sci. Rep.* **9**, 6815. (doi:10.1038/s41598-019-43321-4)
31. Perretti M, Chiang N, La M, Fierro IM, Marullo S, Getting SJ, Solito E, Serhan CN. 2002 Endogenous lipid- and peptide-derived anti-inflammatory pathways generated with glucocorticoid and aspirin treatment activate the lipoxin A4 receptor. *Nat. Med.* **8**, 1296–1302. (doi:10.1038/nm786)
32. Galvao I *et al.* 2020 The role of annexin A1 in the modulation of the NLRP3 inflammasome. *Immunology* **160**, 78–89. (doi:10.1111/imm.13184)
33. Ye RD, Sun L. 2015 Emerging functions of serum amyloid A in inflammation. *J. Leukocyte Biol.* **98**, 923–929. (doi:10.1189/jlb.3VMR0315-080R)
34. Coffelt SB, Tomchuck SL, Zwezdaryk KJ, Danka ES, Scandurro AB. 2009 Leucine leucine-37 uses formyl peptide receptor-like 1 to activate signal transduction pathways, stimulate oncogenic gene expression, and enhance the invasiveness of ovarian cancer cells. *Mol. Cancer Res.* **7**, 907–915. (doi:10.1158/1541-7786.MCR-08-0326)
35. De Paulis A *et al.* 2009 Helicobacter pylori Hp(2-20) promotes migration and proliferation of gastric epithelial cells by interacting with formyl peptide receptors in vitro and accelerates gastric mucosal healing in vivo. *J. Immunol.* **183**, 3761–3769. (doi:10.4049/jimmunol.0900863)
36. Tadei MB, Mayorquim MV, De Souza CB, De Souza Costa S, Possebon L, Souza HR, Iyomasa-Pilon MM, Geromel MR, Girol AP. 2018 Expression of the Annexin A1 and its correlation with matrix metalloproteinases and the receptor for formylated peptide-2 in diffuse astrocytic tumors. *Ann. Diagn. Pathol.* **37**, 62–66. (doi:10.1016/j.anndiagpath.2018.08.002)
37. Zong L *et al.* 2016 Lipoxin A4 attenuates cell invasion by inhibiting ROS/ERK/MMP pathway in pancreatic cancer. *Oxidat. Med. Cell. Longevity* **2016**, 6815727. (doi:10.1155/2016/6815727)
38. Cattaneo F, Russo R, Castaldo M, Chambery A, Zollo C, Esposito G, Pedone PV, Ammendola R. 2019 Phosphoproteomic analysis sheds light on intracellular signaling cascades triggered by formyl-peptide receptor 2. *Sci. Rep.* **9**, 17894. (doi:10.1038/s41598-019-54502-6)
39. Raabe CA, Groper J, Rescher U. 2019 Biased perspectives on formyl peptide receptors. *Biochim. Biophys. Acta Mol. Cell Res.* **1866**, 305–316. (doi:10.1016/j.bbamcr.2018.11.015)
40. Tonks NK. 2005 Redox redux: revisiting PTPs and the control of cell signaling. *Cell* **121**, 667–670. (doi:10.1016/j.cell.2005.05.016)

41. Chiarugi P, Cirri P. 2003 Redox regulation of protein tyrosine phosphatases during receptor tyrosine kinase signal transduction. *Trends Biochem. Sci.* **28**, 509–514. (doi:10.1016/S0968-0004(03)00174-9)
42. Finkel T. 1999 Signal transduction by reactive oxygen species in non-phagocytic cells. *J. Leukocyte Biol.* **65**, 337–340. (doi:10.1002/jlb.65.3.337)
43. Cattaneo F, Parisi M, Ammendola R. 2013 Distinct signaling cascades elicited by different formyl peptide receptor 2 (FPR2) agonists. *Int. J. Mol. Sci.* **14**, 7193–7230. (doi:10.3390/ijms14047193)
44. Annunziata MC, Parisi M, Esposito G, Fabbrocini G, Ammendola R, Cattaneo F. 2020 Phosphorylation sites in protein kinases and phosphatases regulated by formyl peptide receptor 2 signaling. *Int. J. Mol. Sci.* **21**, 3818. (doi:10.3390/ijms21113818)
45. Pecchillo Cimmino T, Pagano E, Stornaiuolo M, Esposito G, Ammendola R, Cattaneo F. 2022 Formyl-peptide receptor 2 signaling redirects glucose and glutamine into anabolic pathways in metabolic reprogramming of lung cancer cells. *Antioxidants* **11**, 1692. (doi:10.3390/antiox11091692)
46. Sommella E *et al.* 2019 A Boost in mitochondrial activity underpins the cholesterol-lowering effect of annurca apple polyphenols on hepatic cells. *Nutrients* **11**, 163. (doi:10.3390/nu11010163)
47. Riccio G *et al.* 2018 Annurca apple polyphenols protect murine hair follicles from taxane induced dystrophy and hijacks polyunsaturated fatty acid metabolism toward beta-oxidation. *Nutrients* **10**, 1808. (doi:10.3390/nu10111808)
48. Badolati N *et al.* 2018 Annurca apple polyphenols ignite keratin production in hair follicles by inhibiting the pentose phosphate pathway and amino acid oxidation. *Nutrients* **10**, 1406. (doi:10.3390/nu10101406)
49. Schiattarella GG *et al.* 2018 Akap1 regulates vascular function and endothelial cells behavior. *Hypertension* **71**, 507–517. (doi:10.1161/HYPERTENSIONAHA.117.10185)
50. Pavone LM, Cattaneo F, Rea S, De Pasquale V, Spina A, Sauchelli E, Mastellone V, Ammendola R. 2011 Intracellular signaling cascades triggered by the NK1 fragment of hepatocyte growth factor in human prostate epithelial cell line PNT1A. *Cell. Signal.* **23**, 1961–1971. (doi:10.1016/j.cellsig.2011.07.005)
51. Koppenol WH, Bounds PL, Dang CV. 2011 Otto Warburg's contributions to current concepts of cancer metabolism. *Nat. Rev. Cancer* **11**, 325–337. (doi:10.1038/nrc3038)
52. Martinez CA, Scafoglio C. 2020 Heterogeneity of glucose transport in lung cancer. *Biomolecules* **10**, 868. (doi:10.3390/biom10060868)
53. Sasaki H, Shitara M, Yokota K, Hikosaka Y, Moriyama S, Yano M, Fujii Y. 2012 Overexpression of GLUT1 correlates with Kras mutations in lung carcinomas. *Mol. Med. Rep.* **5**, 599–602. (doi:10.3892/mmr.2011.736)
54. Osthus RC *et al.* 2000 Deregulation of glucose transporter 1 and glycolytic gene expression by c-Myc. *J. Biol. Chem.* **275**, 21 797–21 800. (doi:10.1074/jbc.C000023200)
55. Barthel A, Okino ST, Liao J, Nakatani K, Li J, Whitlock JP, Roth RA. 1999 Regulation of GLUT1 gene transcription by the serine/threonine kinase Akt1. *J. Biol. Chem.* **274**, 20 281–20 286. (doi:10.1074/jbc.274.29.20281)
56. Barron CC, Bilan PJ, Tsakiridis T, Tsiani E. 2016 Facilitative glucose transporters: implications for cancer detection, prognosis and treatment. *Metabolism Clin. Exp.* **65**, 124–139. (doi:10.1016/j.metabol.2015.10.007)
57. Schwartzenberg-Bar-Yoseph F, Armoni M, Karnieli E. 2004 The tumor suppressor p53 down-regulates glucose transporters GLUT1 and GLUT4 gene expression. *Cancer Res.* **64**, 2627–2633. (doi:10.1158/0008-5472.CAN-03-0846)
58. Wardzala LJ, Jeanrenaud B. 1981 Potential mechanism of insulin action on glucose transport in the isolated rat diaphragm. Apparent translocation of intracellular transport units to the plasma membrane. *J. Biol. Chem.* **256**, 7090–7093. (doi:10.1016/S0021-9258(19)68926-X)
59. Suzuki K, Kono T. 1980 Evidence that insulin causes translocation of glucose transport activity to the plasma membrane from an intracellular storage site. *Proc. Natl Acad. Sci. USA* **77**, 2542–2545. (doi:10.1073/pnas.77.5.2542)
60. Mcbrayer SK, Cheng JC, Singhal S, Krett NL, Rosen ST, Shanmugam M. 2012 Multiple myeloma exhibits novel dependence on GLUT4, GLUT8, and GLUT11: implications for glucose transporter-directed therapy. *Blood* **119**, 4686–4697. (doi:10.1182/blood-2011-09-377846)
61. Shibata K, Kajiyama H, Mizokami Y, Ino K, Nomura S, Mizutani S, Terauchi M, Kikkawa F. 2005 Placental leucine aminopeptidase (P-LAP) and glucose transporter 4 (GLUT4) expression in benign, borderline, and malignant ovarian epithelia. *Gynecol. Oncol.* **98**, 11–18. (doi:10.1016/j.ygyno.2005.03.043)
62. Mao A, Zhou X, Liu Y, Ding J, Miao A, Pan G. 2019 KLF8 is associated with poor prognosis and regulates glycolysis by targeting GLUT4 in gastric cancer. *J. Cell. Mol. Med.* **23**, 5087–5097. (doi:10.1111/jcmm.14378)
63. Hou N *et al.* 2019 Carvacrol attenuates diabetic cardiomyopathy by modulating the PI3K/AKT/GLUT4 pathway in diabetic mice. *Front. Pharmacol.* **10**, 998. (doi:10.3389/fphar.2019.00998)
64. Cattaneo F, Guerra G, Ammendola R. 2010 Expression and signaling of formyl-peptide receptors in the brain. *Neurochem. Res.* **35**, 2018–2026. (doi:10.1007/s11064-010-0301-5)
65. Hernandez-Sanchez C, Blakesley V, Kalebic T, Helman L, Leroith D. 1995 The role of the tyrosine kinase domain of the insulin-like growth factor-I receptor in intracellular signaling, cellular proliferation, and tumorigenesis. *J. Biol. Chem.* **270**, 29 176–29 181. (doi:10.1074/jbc.270.49.29176)
66. Lopaczynski W, Terry C, Nissley P. 2000 Autophosphorylation of the insulin-like growth factor I receptor cytoplasmic domain. *Biochem. Biophys. Res. Commun.* **279**, 955–960. (doi:10.1006/bbrc.2000.4046)
67. Lemarie A, Bourdonnay E, Morzadec C, Fardel O, Vernhet L. 2008 Inorganic arsenic activates reduced NADPH oxidase in human primary macrophages through a Rho kinase/p38 kinase pathway. *J. Immunol.* **180**, 6010–6017. (doi:10.4049/jimmunol.180.9.6010)
68. Mora-Pale M, Weiwer M, Yu J, Linhardt RJ, Dordick JS. 2009 Inhibition of human vascular NADPH oxidase by apocynin derived oligophenols. *Bioorg. Med. Chem.* **17**, 5146–5152. (doi:10.1016/j.bmc.2009.05.061)
69. Fischer OM, Giordano S, Comoglio PM, Ullrich A. 2004 Reactive oxygen species mediate Met receptor transactivation by G protein-coupled receptors and the epidermal growth factor receptor in human carcinoma cells. *J. Biol. Chem.* **279**, 28 970–28 978. (doi:10.1074/jbc.M402508200)
70. Catarzi S, Biagioni C, Giannoni E, Favilli F, Marcucci T, Iantomasi T, Vincenzini MT. 2005 Redox regulation of platelet-derived-growth-factor-receptor: role of NADPH-oxidase and c-Src tyrosine kinase. *Biochim. Biophys. Acta* **1745**, 166–175. (doi:10.1016/j.bbamcr.2005.03.004)
71. Bae YS, Kang SW, Seo MS, Baines IC, Tekle E, Chock PB, Rhee SG. 1997 Epidermal growth factor (EGF)-induced generation of hydrogen peroxide. Role in EGF receptor-mediated tyrosine phosphorylation. *J. Biol. Chem.* **272**, 217–221. (doi:10.1074/jbc.272.1.217)
72. Sundaresan M, Yu ZX, Ferrans VJ, Irani K, Finkel T. 1995 Requirement for generation of H_2O_2 for platelet-derived growth factor signal transduction. *Science* **270**, 296–299. (doi:10.1126/science.270.5234.296)
73. Deberardinis RJ, Chandel NS. 2016 Fundamentals of cancer metabolism. *Sci. Adv.* **2**, e1600200. (doi:10.1126/sciadv.1600200)
74. Okar DA, Manzano A, Navarro-Sabate A, Riera L, Bartrons R, Lange AJ. 2001 PFK-2/FBPase-2: maker and breaker of the essential biofactor fructose-2,6-bisphosphate. *Trends Biochem. Sci.* **26**, 30–35. (doi:10.1016/S0968-0004(00)01699-6)
75. Ozcan SC *et al.* 2020 PFKFB2 regulates glycolysis and proliferation in pancreatic cancer cells. *Mol. Cell. Biochem.* **470**, 115–129. (doi:10.1007/s11010-020-03751-5)
76. Lee M *et al.* 2020 Mutation of regulatory phosphorylation sites in PFKFB2 worsens renal fibrosis. *Sci. Rep.* **10**, 14531. (doi:10.1038/s41598-020-71475-z)
77. Minchenko O, Opentanova I, Caro J. 2003 Hypoxic regulation of the 6-phosphofructo-2-kinase/fructose-2,6-bisphosphatase gene family (PFKFB-1-4) expression in vivo. *FEBS Lett.* **554**, 264–270. (doi:10.1016/S0014-5793(03)01179-7)
78. Rider MH, Bertrand L, Vertommen D, Michels PA, Rousseau GG, Hue L. 2004 6-Phosphofructo-2-kinase/fructose-2,6-bisphosphatase: head-to-head with a bifunctional enzyme that controls glycolysis. *Biochem. J.* **381**, 561–579. (doi:10.1042/BJ20040752)
79. Mouton V *et al.* 2010 Heart 6-phosphofructo-2-kinase activation by insulin requires PKB (protein kinase B), but not SGK3 (serum- and glucocorticoid-

induced protein kinase 3). *Biochem. J.* **431**, 267–275. (doi:10.1042/BJ20101089)

80. Sabbatini P *et al.* 2009 Antitumor activity of GSK1904529A, a small-molecule inhibitor of the insulin-like growth factor-I receptor tyrosine kinase. *Clin. Cancer Res.* **15**, 3058–3067. (doi:10.1158/1078-0432.CCR-08-2530)
81. Michael M *et al.* 2017 A phase 1 study of LY2874455, an oral selective pan-FGFR inhibitor, in patients with advanced cancer. *Targeted Oncol.* **12**, 463–474. (doi:10.1007/s11523-017-0502-9)
82. Zhu X-F, Liu Z-C, Xie B-F, Li Z-M, Feng G-K, Yang D, Zeng Y-X. 2001 EGFR tyrosine kinase inhibitor AG1478 inhibits cell proliferation and arrests cell cycle in nasopharyngeal carcinoma cells. *Cancer Lett.* **169**, 27–32. (doi:10.1016/S0304-3835(01)00547-X)
83. Eswarakumar VP, Lax I, Schlessinger J. 2005 Cellular signaling by fibroblast growth factor receptors. *Cytokine Growth Factor Rev.* **16**, 139–149. (doi:10.1016/j.cytogfr.2005.01.001)
84. Ornitz DM, Itoh N. 2015 The fibroblast growth factor signaling pathway. *Wiley Interdiscipl. Rev. Develop. Biol.* **4**, 215–266. (doi:10.1002/wdev.176)
85. Kouhara H, Hadari YR, Spivak-Kroizman T, Schilling J, Bar-Sagi D, Lax I, Schlessinger J. 1997 A lipid-anchored Grb2-binding protein that links FGF-receptor activation to the Ras/MAPK signaling pathway. *Cell* **89**, 693–702. (doi:10.1016/S0092-8674(00)80252-4)
86. Hadari YR, Kouhara H, Lax I, Schlessinger J. 1998 Binding of Shp2 tyrosine phosphatase to FRS2 is essential for fibroblast growth factor-induced PC12 cell differentiation. *Mol. Cell. Biol.* **18**, 3966–3973. (doi:10.1128/MCB.18.7.3966)
87. Zhang K *et al.* 2013 Amplification of FRS2 and activation of FGFR/FRS2 signaling pathway in high-grade liposarcoma. *Cancer Res.* **73**, 1298–1307. (doi:10.1158/0008-5472.CAN-12-2086)
88. Patel MS, Korotchkina LG. 2006 Regulation of the pyruvate dehydrogenase complex. *Biochem. Soc. Trans.* **34**(Pt 2), 217–222. (doi:10.1042/BST0340217)
89. Roche TE, Hiromasa Y. 2007 Pyruvate dehydrogenase kinase regulatory mechanisms and inhibition in treating diabetes, heart ischemia, and cancer. *Cell. Mol. Life Sci.* **64**, 830–849. (doi:10.1007/s00018-007-6380-z)
90. Hiromasa Y, Fujisawa T, Aso Y, Roche TE. 2004 Organization of the cores of the mammalian pyruvate dehydrogenase complex formed by E2 and E2 plus the E3-binding protein and their capacities to bind the E1 and E3 components. *J. Biol. Chem.* **279**, 6921–6933. (doi:10.1074/jbc.M308172200)
91. Mcfate T *et al.* 2008 Pyruvate dehydrogenase complex activity controls metabolic and malignant phenotype in cancer cells. *J. Biol. Chem.* **283**, 22 700–22 708. (doi:10.1074/jbc.M801765200)
92. Sugden MC, Holness MJ. 2006 Mechanisms underlying regulation of the expression and activities of the mammalian pyruvate dehydrogenase kinases. *Arch. Physiol. Biochem.* **112**, 139–149. (doi:10.1080/13813450600935263)
93. Hitosugi T *et al.* 2011 Tyrosine phosphorylation of mitochondrial pyruvate dehydrogenase kinase 1 is important for cancer metabolism. *Mol. Cell* **44**, 864–877. (doi:10.1016/j.molcel.2011.10.015)
94. Shan C *et al.* 2014 Tyr-94 phosphorylation inhibits pyruvate dehydrogenase phosphatase 1 and promotes tumor growth. *J. Biol. Chem.* **289**, 21 413–21 422. (doi:10.1074/jbc.M114.581124)
95. Luo F, Li Y, Yuan F, Zuo J. 2019 Hexokinase II promotes the Warburg effect by phosphorylating alpha subunit of pyruvate dehydrogenase. *Chin. J. Cancer Res.* **31**, 521–532. (doi:10.21147/j.issn.1000-9604.2019.03.14)
96. Kim H, Park SH, Han SY, Lee YS, Cho J, Kim JM. 2020 LXA(4)-FPR2 signaling regulates radiation-induced pulmonary fibrosis via crosstalk with TGF-beta/Smad signaling. *Cell Death Dis.* **11**, 653. (doi:10.1038/s41419-020-02846-7)
97. Wymann MP, Marone R. 2005 Phosphoinositide 3-kinase in disease: timing, location, and scaffolding. *Curr. Opin. Cell Biol.* **17**, 141–149. (doi:10.1016/j.ceb.2005.02.011)
98. Cantley LC. 2002 The phosphoinositide 3-kinase pathway. *Science* **296**, 1655–1657. (doi:10.1126/science.296.5573.1655)
99. Chae YC *et al.* 2016 Mitochondrial Akt regulation of hypoxic tumor reprogramming. *Cancer Cell* **30**, 257–272. (doi:10.1016/j.ccell.2016.07.004)
100. Brown DI, Griendling KK. 2009 Nox proteins in signal transduction. *Free Rad. Biol. Med.* **47**, 1239–1253. (doi:10.1016/j.freeradbiomed.2009.07.023)
101. Esposito G, Carsana A. 2019 Metabolic alterations in cardiomyocytes of patients with Duchenne and Becker muscular dystrophies. *J. Clin. Med.* **8**, 2151. (doi:10.3390/jcm8122151)
102. Paoli P, Giannoni E, Chiarugi P. 2013 Anoikis molecular pathways and its role in cancer progression. *Biochim. Biophys. Acta* **1833**, 3481–3498. (doi:10.1016/j.bbamcr.2013.06.026)
103. Groeger G, Quiney C, Cotter TG. 2009 Hydrogen peroxide as a cell-survival signaling molecule. *Antioxid. Redox Signal* **11**, 2655–2671. (doi:10.1089/ars.2009.2728)
104. Bui T, Thompson CB. 2006 Cancer's sweet tooth. *Cancer Cell* **9**, 419–420. (doi:10.1016/j.ccr.2006.05.012)
105. Fan J *et al.* 2011 Tyrosine phosphorylation of lactate dehydrogenase A is important for NADH/NAD(+) redox homeostasis in cancer cells. *Mol. Cell. Biol.* **31**, 4938–4950. (doi:10.1128/MCB.06120-11)
106. Liu J *et al.* 2018 Aberrant FGFR tyrosine kinase signaling enhances the Warburg effect by reprogramming LDH isoform expression and activity in prostate cancer. *Cancer Res.* **78**, 4459–4470. (doi:10.1158/0008-5472.CAN-17-3226)
107. Jin L *et al.* 2017 Phosphorylation-mediated activation of LDHA promotes cancer cell invasion and tumour metastasis. *Oncogene* **36**, 3797–3806. (doi:10.1038/onc.2017.6)
108. Sandilands E, Akbarzadeh S, Vecchione A, Mcewan DG, Frame MC, Heath JK. 2007 Src kinase modulates the activation, transport and signalling dynamics of fibroblast growth factor receptors. *EMBO Rep.* **8**, 1162–1169. (doi:10.1038/sj.embor.7401097)
109. Ren M, Qin H, Ren R, Tidwell J, Cowell JK. 2011 Src activation plays an important key role in lymphomagenesis induced by FGFR1 fusion kinases. *Cancer Res.* **71**, 7312–7322. (doi:10.1158/0008-5472.CAN-11-1109)
110. Zdralevic M, Vucetic M, Daher B, Marchiq I, Parks SK, Pouyssegur J. 2018 Disrupting the 'Warburg effect' re-routes cancer cells to OXPHOS offering a vulnerability point via 'ferroptosis'-induced cell death. *Adv. Biol. Reg.* **68**, 55–63. (doi:10.1016/j.jbior.2017.12.002)
111. Dang CV, Le A, Gao P. 2009 MYC-induced cancer cell energy metabolism and therapeutic opportunities. *Clin. Cancer Res.* **15**, 6479–6483. (doi:10.1158/1078-0432.CCR-09-0889)
112. Dabral S *et al.* 2019 A RASSF1A-HIF1alpha loop drives Warburg effect in cancer and pulmonary hypertension. *Nat. Commun.* **10**, 2130. (doi:10.1038/s41467-019-10044-z)
113. Hirota K. 2021 HIF-alpha prolyl hydroxylase inhibitors and their implications for biomedicine: a comprehensive review. *Biomedicines* **9**, 468. (doi:10.3390/biomedicines9050468)
114. Semenza GL. 2010 HIF-1: upstream and downstream of cancer metabolism. *Cur. Opin. Genet. Dev.* **20**, 51–56. (doi:10.1016/j.gde.2009.10.009)
115. Seo HR, Kim J, Bae S, Soh JW, Lee YS. 2008 Cdk5-mediated phosphorylation of c-Myc on Ser-62 is essential in transcriptional activation of cyclin B1 by cyclin G1. *J. Biol. Chem.* **283**, 15 601–15 610. (doi:10.1074/jbc.M800987200)
116. Jeong YS, Bae YS. 2020 Formyl peptide receptors in the mucosal immune system. *Exp. Mol. Med.* **52**, 1694–1704. (doi:10.1038/s12276-020-00518-2)
117. Wang L, Hayashi H, Kishi K, Huang L, Hagi A, Tamaoka K, Hawkins PT, Ebina Y. 2000 Gi-mediated translocation of GLUT4 is independent of p85/p110alpha and p110gamma phosphoinositide 3-kinases but might involve the activation of Akt kinase. *Biochem. J.* **345**, 543–555. (doi:10.1042/bj3450543)
118. Malide D, Davies-Hill TM, Levine M, Simpson IA. 1998 Distinct localization of GLUT-1, -3, and -5 in human monocyte-derived macrophages: effects of cell activation. *Am. J. Physiol.* **274**, E516–E526.
119. Ahmed N, Kansara M, Berridge MV. 1997 Acute regulation of glucose transport in a monocyte-macrophage cell line: Glut-3 affinity for glucose is enhanced during the respiratory burst. *Biochem. J.* **327**, 369–375. (doi:10.1042/bj3270369)
120. Tu H, Xu C, Zhang W, Liu Q, Rondard P, Pin J-P, Liu J. 2010 GABAB receptor activation protects neurons from apoptosis via IGF-1 receptor transactivation. *J. Neurosci.* **30**, 749–759. (doi:10.1523/JNEUROSCI.2343-09.2010)
121. Du J, Brink M, Peng T, Mottironi B, Delafontaine P. 2001 Thrombin regulates insulin-like growth factor-1 receptor transcription in vascular smooth muscle: characterization of the signaling pathway. *Circ. Res.* **88**, 1044–1052. (doi:10.1161/hh1001.090840)

122. Teh JLF, Shah R, Shin S, Wen Y, Mehnert JM, Goydos J, Chen S. 2014 Metabotropic glutamate receptor 1 mediates melanocyte transformation via transactivation of insulin-like growth factor 1 receptor. *Pigment Cell Melanoma Res.* **27**, 621–629. (doi:10.1111/pcmr.12237)
123. Zhao D, Bakirtzi K, Zhan Y, Zeng H, Koon HW, Pothoulakis C. 2011 Insulin-like growth factor-1 receptor transactivation modulates the inflammatory and proliferative responses of neurotensin in human colonic epithelial cells. *J. Biol. Chem.* **286**, 6092–6099. (doi:10.1074/jbc.M110.192534)
124. Zahradka P, Litchie B, Storie B, Helwer G. 2004 Transactivation of the insulin-like growth factor-I receptor by angiotensin II mediates downstream signaling from the angiotensin II type 1 receptor to phosphatidylinositol 3-kinase. *Endocrinology* **145**, 2978–2987. (doi:10.1210/en.2004-0029)
125. Di Liberto V, Mudo G, Belluardo N. 2019 Crosstalk between receptor tyrosine kinases (RTKs) and G protein-coupled receptors (GPCR) in the brain: focus on heteroreceptor complexes and related functional neurotrophic effects. *Neuropharmacology* **152**, 67–77. (doi:10.1016/j.neuropharm.2018.11.018)
126. Flajolet M *et al.* 2008 FGF acts as a co-transmitter through adenosine A(2A) receptor to regulate synaptic plasticity. *Nat. Neurosci.* **11**, 1402–1409. (doi:10.1038/nn.2216)
127. Asimaki O, Leondaritis G, Lois G, Sakellaridis N, Mangoura D. 2011 Cannabinoid 1 receptor-dependent transactivation of fibroblast growth factor receptor 1 emanates from lipid rafts and amplifies extracellular signal-regulated kinase 1/2 activation in embryonic cortical neurons. *J. Neurochem.* **116**, 866–873. (doi:10.1111/j.1471-4159.2010.07030.x)
128. Narváez M, Andrade-Talavera Y, Valladolid-Acebes I, Fredriksson M, Siegele P, Hernandez-Sosa A, Fisahn A, Fuxe K, Borroto-Escuela DO. 2020 Existence of FGFR1-5-HT1AR heteroreceptor complexes in hippocampal astrocytes. Putative link to 5-HT and FGF2 modulation of hippocampal gamma oscillations. *Neuropharmacology* **170**, 108070. (doi:10.1016/j.neuropharm.2020.108070)
129. Borroto-Escuela DO *et al.* 2015 Evidence for the existence of FGFR1-5-HT1A heteroreceptor complexes in the midbrain raphe 5-HT system. *Biochem. Biophys. Res. Commun.* **456**, 489–493. (doi:10.1016/j.bbrc.2014.11.112)
130. Di Liberto V, Borroto-Escuela DO, Frinchi M, Verdi V, Fuxe K, Belluardo N, Mudò G. 2017 Existence of muscarinic acetylcholine receptor (mAChR) and fibroblast growth factor receptor (FGFR) heteroreceptor complexes and their enhancement of neurite outgrowth in neural hippocampal cultures. *Biochim. Biophys. Acta Gen.* **1861**, 235–245. (doi:10.1016/j.bbagen.2016.10.026)
131. Belcheva MM, Haas PD, Tan Y, Heaton VM, Coscia CJ. 2002 The fibroblast growth factor receptor is at the site of convergence between mu-opioid receptor and growth factor signaling pathways in rat C6 glioma cells. *J. Pharmacol. Exp. Ther.* **303**, 909–918. (doi:10.1124/jpet.102.038554)
132. Yu Y *et al.* 2017 The G-protein-coupled chemoattractant receptor Fpr2 exacerbates high glucose-mediated proinflammatory responses of Muller glial cells. *Front. Immunol.* **8**, 1852. (doi:10.3389/fimmu.2017.01852)
133. Terzuoli E, Corti F, Nannelli G, Giachetti A, Donnini S, Ziche M. 2018 Bradykinin B2 receptor contributes to inflammatory responses in human endothelial cells by the transactivation of the fibroblast growth factor receptor FGFR-1. *Int. J. Mol. Sci.* **19**, 2638. (doi:10.3390/ijms19092638)
134. Goetze K, Walenta S, Ksiazkiewicz M, Kunz-Schughart LA, Mueller-Klieser W. 2011 Lactate enhances motility of tumor cells and inhibits monocyte migration and cytokine release. *Int. J. Oncol.* **39**, 453–463. (doi:10.3892/ijo.2011.1055)
135. Ahmed K, Tunaru S, Tang C, Müller M, Gille A, Sassmann A, Hanson J, Offermanns S. 2010 An autocrine lactate loop mediates insulin-dependent inhibition of lipolysis through GPR81. *Cell Metab.* **11**, 311–319. (doi:10.1016/j.cmet.2010.02.012)
136. Roland CL *et al.* 2014 Cell surface lactate receptor GPR81 is crucial for cancer cell survival. *Cancer Res.* **74**, 5301–5310. (doi:10.1158/0008-5472.CAN-14-0319)
137. Lee YJ *et al.* 2016 G-protein-coupled receptor 81 promotes a malignant phenotype in breast cancer through angiogenic factor secretion. *Oncotarget* **7**, 70 898–70 911. (doi:10.18632/oncotarget.12286)
138. Fantin VR, St-Pierre J, Leder P. 2006 Attenuation of LDH-A expression uncovers a link between glycolysis, mitochondrial physiology, and tumor maintenance. *Cancer Cell.* **9**, 425–434. (doi:10.1016/j.ccr.2006.04.023)
139. Eichenlaub T *et al.* 2018 Warburg effect metabolism drives neoplasia in a Drosophila genetic model of epithelial cancer. *Curr. Biol.* **28**, 3220–8 e6. (doi:10.1016/j.cub.2018.08.035)
140. Vander Heiden MG, Cantley LC, Thompson CB. 2009 Understanding the Warburg effect: the metabolic requirements of cell proliferation. *Science* **324**, 1029–1033. (doi:10.1126/science.1160809)
141. Levine AJ, Puzio-Kuter AM. 2010 The control of the metabolic switch in cancers by oncogenes and tumor suppressor genes. *Science* **330**, 1340–1344. (doi:10.1126/science.1193494)
142. Deberardinis RJ, Lum JJ, Hatzivassiliou G, Thompson CB. 2008 The biology of cancer: metabolic reprogramming fuels cell growth and proliferation. *Cell Metab.* **7**, 11–20. (doi:10.1016/j.cmet.2007.10.002)
143. Boroughs LK, Deberardinis RJ. 2015 Metabolic pathways promoting cancer cell survival and growth. *Nat. Cell Biol.* **17**, 351–359. (doi:10.1038/ncb3124)
144. Lunt SY, Vander Heiden MG. 2011 Aerobic glycolysis: meeting the metabolic requirements of cell proliferation. *Ann. Rev. Cell Devel. Biol.* **27**, 441–464. (doi:10.1146/annurev-cellbio-092910-154237)
145. Dang CV, Kim JW, Gao P, Yustein J. 2008 The interplay between MYC and HIF in cancer. *Nat. Rev. Cancer* **8**, 51–56. (doi:10.1038/nrc2274)
146. Sakagami H *et al.* 2014 Loss of HIF-1alpha impairs GLUT4 translocation and glucose uptake by the skeletal muscle cells. *Am. J. Physiol. Endocrinol. Metab.* **306**, E1065–E1076. (doi:10.1152/ajpendo.00597.2012)
147. HenríQuez-Olguin C *et al.* 2019 Cytosolic ROS production by NADPH oxidase 2 regulates muscle glucose uptake during exercise. *Nat. Commun.* **10**, 4623. (doi:10.1038/s41467-019-12523-9)
148. Cruzado MC, Risler NR, Miatello RM, Yao G, Schiffrin EL, Touyz RM. 2005 Vascular smooth muscle cell NAD(P)H oxidase activity during the development of hypertension: effect of angiotensin II and role of insulinlike growth factor-1 receptor transactivation. *Am. J. Hypertens.* **18**, 81–87. (doi:10.1016/j.amjhyper.2004.09.001)
149. Cesi G, Walbrecq G, Zimmer A, Kreis S, Haan C. 2017 ROS production induced by BRAF inhibitor treatment rewires metabolic processes affecting cell growth of melanoma cells. *Mol. Cancer* **16**, 102. (doi:10.1186/s12943-017-0667-y)
150. Woolbright BL, Rajendran G, Harris RA, Taylor 3rd JA. 2019 Metabolic flexibility in cancer: targeting the pyruvate dehydrogenase kinase:pyruvate dehydrogenase axis. *Mol. Cancer Ther.* **18**, 1673–1681. (doi:10.1158/1535-7163.MCT-19-0079)
151. Zhang M *et al.* 2010 NADPH oxidase-4 mediates protection against chronic load-induced stress in mouse hearts by enhancing angiogenesis. *Proc. Natl Acad. Sci. USA* **107**, 18 121–18 126. (doi:10.1073/pnas.1009700107)
152. Cadenas S. 2018 ROS and redox signaling in myocardial ischemia-reperfusion injury and cardioprotection. *Free Rad. Biol. Med.* **117**, 76–89. (doi:10.1016/j.freeradbiomed.2018.01.024)
153. Goyal P *et al.* 2004 Upregulation of NAD(P)H oxidase 1 in hypoxia activates hypoxia-inducible factor 1 via increase in reactive oxygen species. *Free Rad. Biol. Med.* **36**, 1279–1288. (doi:10.1016/j.freeradbiomed.2004.02.071)
154. Diebold I, Flügel D, Becht S, BelAiba RS, Bonello S, Hess J, Kietzmann T, Görlach A. 2010 The hypoxia-inducible factor-2alpha is stabilized by oxidative stress involving NOX4. *Antioxid. Redox Signal.* **13**, 425–436. (doi:10.1089/ars.2009.3014)
155. Diebold I, Petry A, Hess J, Gorlach A. 2010 The NADPH oxidase subunit NOX4 is a new target gene of the hypoxia-inducible factor-1. *Mol. Biol. Cell* **21**, 2087–2096. (doi:10.1091/mbc.e09-12-1003)
156. Cimmino TP, Pagano E, Stornaiuolo M, Esposito G, Ammendola R, Cattaneo F. 2023 Formyl-peptide receptor 2 signalling triggers aerobic metabolism of glucose through Nox2-dependent modulation of pyruvate dehydrogenase activity. Figshare. (doi:10.6084/m9.figshare.c.6875416)